AEDC-TR-73-61

TRANSONIC SCALING EFFECT ON A QUASI, TWO-DIMENSIONAL C-141 AIRFOIL MODEL

C. F. Lo and W. E. Carleton

ARO, Inc.

June 1973

PROPULSION WIND TUNNEL FACILITY
ARNOLD ENGINEERING DEVELOPMENT CENTER
AIR FORCE SYSTEMS COMMAND
ARNOLD AIR FORCE STATION, TENNESSEE

NOTICES

When U. S. Government drawings specifications, or other data are used for any purpose other than a definitely related Government procurement operation, the Government thereby incurs no responsibility nor any obligation whatsoever, and the fact that the Government may have formulated, furnished, or in any way supplied the said drawings, specifications or other data, is not to be regarded by implication or otherwise, or in any manner licensing the holder or any other person or corporation, or conveying any rights or permission to manufacture, use, or sell any patented invention that may in any way be related thereto.

Qualified users may obtain copies of this report from the Defense Documentation Center.

References to named commercial products in this report are not to be considered in any sense as an endorsement of the product by the United States Air Force or the Government.

TRANSONIC SCALING EFFECT ON A QUASI, TWO-DIMENSIONAL C-141 AIRFOIL MODEL

C. F. Lo and W. E. Carleton
ARO, Inc.

FOREWORD

The work reported herein was conducted at the Arnold Engineering Development Center (AEDC), Air Force Systems Command (AFSC), Arnold Air Force Station, Tennessee, under joint sponsorship with the Aerospace Research Laboratories (ARL), AFSC, under Program Elements 64719F and 61102F.

The results presented herein were obtained by ARO, Inc. (a subsidiary of Sverdrup & Parcel and Associates, Inc.), contract operator of AEDC. The research was conducted from February 1970 to June 1972 under ARO Project Nos. PW3087, PW3110, and PW5210, and the manuscript was submitted for publication on January 30, 1972.

This technical report has been reviewed and is approved.

CARLOS TIRRES
Captain, USAF
Research & Development Division
Directorate of Technology

ROBERT O. DIETZ
Director of Technology

ABSTRACT

The transonic scaling effect of shock wave/boundary-layer interaction on a quasi, two-dimensional C-141 airfoil was investigated. Data were obtained from the AEDC Propulsion Wind Tunnel Facility Aerodynamic Wind Tunnel (4T) and Propulsion Wind Tunnel (16T) and from the NASA Marshall Space Flight Center High Reynolds Number Tunnel with 6-in.- and 24-in.-chord airfoils for a range of chord Reynolds numbers from 0.3 to 42 million and Mach numbers from 0.70 to 0.85. In addition to the investigation of the effect of Reynolds number on the airfoil pressure distribution, the effect of fixed boundary-layer transition was evaluated using grit-type transition strips on the airfoil surface. The significant parameters affecting the shock wave/boundary-layer interaction are identified. The data indicate that simulation of higher Reynolds number data on the C-141 airfoil model is feasible by use of a fixed-boundary-layer-transition strip.

CONTENTS

APPENDIXES

I. ILLUSTRATIONS

Figure

Figure Page

NOMENCLATURE

C_p	Pressure coefficient, $(P_\ell - P)/q$
C_p^*	Critical pressure coefficient corresponding to sonic flow on the airfoil surface
c	Airfoil chord length
M_∞	Free-stream Mach number
P	Free-stream static pressure, psfa
P_L	Pressure orifices on lower airfoil surface

P_ℓ	Local surface static pressure, psfa
P_U	Pressure orifices on upper airfoil surfaces
q	Free-stream dynamic pressure, 0.7 P M^2, psf
R	Free-stream unit Reynolds number per foot
R_c	Chord Reynolds number
X, X'	Airfoil chordwise dimension (see Figs. 3 and 4), in.
x_s	Distance of normal shock location on airfoil from airfoil leading edge, in.
x_t	Distance of fixed boundary-layer transition location from airfoil leading edge, in.
Y, Y'	Airfoil spanwise dimension (see Figs. 3 and 4), in.
Z, Z'	Airfoil thickness dimension (see Figs. 3 and 4), in.
α	Airfoil angle of attack measured as the angle between the centerline of the test section and the airfoil x-coordinate reference line
τ	Test section wall porosity, percent open area

SECTION I
INTRODUCTION

A large scaling effect on the phenomena of the shock wave/boundary-layer interaction on airfoils in the transonic regime has recently been revealed (Refs. 1-4). To study the phenomena, an adequately high Reynolds number tunnel is necessary in order to obtain full-scale flight aerodynamic data. Until such a test facility becomes available, however, the substantial portion of future aircraft development testing will have to be conducted in the low Reynolds number tunnels. Even when the Ludwieg or blow-down type of higher Reynolds number tunnels become available in the near future, their low productivity will not allow fulfillment of the large tunnel test hour requirements on the order of 10,000 to 15,000 tunnel hours in the development of a modern commercial transport (Ref. 5). For military aircraft, the requirement of tunnel hours may be even greater than this because of the complexity of their missions. Hence, there is an urgent need to develop the simulation of high Reynolds number testing in existing transonic tunnels.

Several methods have been attempted to simulate high Reynolds number conditions in low Reynolds number tunnels. One of the methods is to adjust the boundary-layer thickness by fixing the transition point to a proper location on the airfoil (Ref. 3). This method is successfully applied on a NASA 65-213 airfoil (Ref. 6). However, it fails when applied to an airfoil with a peaky type of pressure distribution which induces a laminar separation on the forward portion of the airfoil (Ref. 7). This indicates that a general technique for application to all flow situations is questionable and that a better understanding of the complex shock wave/boundary-layer interaction phenomena is needed.

The purpose of this investigation is to advance the basic understanding of the phenomena of the shock wave/boundary-layer interaction, to identify the significant parameters, and to determine the feasibility of high Reynolds number simulation.

The C-141 wing and supercritical wing airfoil sections were chosen to represent the wings of a transport aircraft and a military fighter, respectively. Airfoil pressure data obtained for a large range of Reynolds numbers using two different size airfoils in three transonic wind tunnels are used to study the effects of Reynolds number on the airfoil pressure distribution and to determine the important parameters which influence

the scaling effect. The effects of fixed boundary-layer transition location are investigated at various Reynolds numbers to determine the applicability of fixed transition for high Reynolds number simulation.

In this report, the results for the C-141 airfoil are presented and analyzed, and scaling criteria are suggested. The investigation of the supercritical wing will be reported separately.

SECTION II
MODELS AND SUPPORT SYSTEMS

The investigation was restricted to a two-dimensional airfoil in order to avoid the complicated phenomena in three-dimensional flow. The end-plate type of support system was used to accommodate the two-dimensional airfoil test. Two different chord airfoils, 6-in. and 24-in., with their properly scaled support system, were selected to cover the wide range of chord Reynolds numbers, R_c, from 0.5×10^6 to 11×10^6 in the Propulsion Wind Tunnel Facility Aerodynamic Wind Tunnel (4T) and Propulsion Wind Tunnel (16T). The 6-in.-chord airfoil was also tested in the NASA Marshall Space Flight Center (MSFC) High Reynolds Number Tunnel (NASA-HRNT) to cover the chord Reynolds numbers from 6×10^6 to 41×10^6.

The sketches showing details of the quasi, two-dimensional airfoil support hardware and the airfoil section for the 6-in.-chord airfoil and the 24-in.-chord airfoil are presented in Figs. 1 and 2 (Appendix I), respectively. Pressure orifice locations for the 6-in.-chord airfoil and the 24-in.-chord airfoil are presented in Figs. 3 and 4, respectively. The airfoil model is a two-dimensional simulation of the airfoil cross section at the 38.9-percent semispan of the C-141 airplane as described in Figs. 3 and 4. Airfoil section coordinates of the model are presented in Table 1 (Appendix II).

The 6-in.-chord airfoil model and support system were designed and constructed of high-strength steel for the test in the NASA-HRNT. The maximum cross-sectional areas at planes through the maximum thicknesses of the airfoil and the rear support hardware are approximately 18 $in.^2$ and 60 $in.^2$, respectively. Stainless steel, 0.066-in.-I.D. tubes are embedded in the upper and lower surfaces of the airfoil model along the airfoil chord, and five 0.030-in. holes are connected through the airfoil surface into each pressure tube, as depicted in Fig.

3. The airfoil model had provisions for mounting a static pressure measuring probe on the side of the end plates, as shown in Fig. 5.

The 24-in.-chord airfoil model and support hardware were designed four times the scale of the 6-in. chord airfoil model and support hardware. The airfoil model and rear support were constructed of steel, and the side plates were constructed of aluminum. Fairings were used on the rear support as shown in Figs. 2 and 6 to obtain the 4-times scale of the rear support of the 6-in. chord model. The maximum cross-sectional areas at planes through the maximum thicknesses of the airfoil and the rear support with fairings are approximately 72 $in.^2$ and 240 $in.^2$, respectively.

SECTION III
TEST FACILITIES AND INSTRUMENTATION

3.1 TUNNEL 4T

Tunnel 4T is a closed-loop, continuous flow, variable density wind tunnel capable of operating at Mach numbers from 0.20 to 1.30. The tunnel stagnation pressure can be varied from approximately 200 to 3400 psfa. The test section is 4 ft. square and 12.5 ft. long with perforated, variable porosity (0.5 to 10 percent) walls. A photograph showing the model installed in the test section and a schematic of the test section showing details of the variable porosity walls and the location of the model are presented in Figs. 5 and 7, respectively. A complete description of the tunnel may be found in Ref. 8.

3.2 TUNNEL 16T

Tunnel 16T is a closed-loop, continuous flow tunnel capable of operation at Mach numbers from 0.20 to 1.60 and at stagnation pressures from approximately 100 to 4000 psfa. The test section is 16 ft. square by 40 ft. long with perforated walls of 6-percent porosity. A schematic of the test section showing wall details and the location of the 6-in.-chord model and a photograph showing the model installed in the test section are presented in Figs. 8 and 9, respectively. The auxiliary pitch mechanism shown in Figs. 8 and 9 was used only as a sting adaptor, and not for pitching the model. A photograph showing the model installed in the test section and a schematic of the test section showing

details of the installation of the 24-in.-chord model are presented in Figs. 6 and 10, respectively. The model restraining cables were attached very near the model 1/4-chord location (center-of-pitch location) to prohibit model translation. A complete description of the tunnel may be found in Ref. 8.

3.3 NASA-HIGH REYNOLDS NUMBER TUNNEL

The NASA Marshall Space Flight Center High Reynolds Number Tunnel is capable of operating at charge pressures of approximately 30 to 715 psia for Mach numbers 0.2 to 2.0. The tube tunnel has provisions for installing various test sections and nozzles for operating throughout the Mach number range.

A test section with perforated walls of variable porosity (0 to 10 percent), a variable-area ejector orifice located at the downstream end of the plenum chamber surrounding the test section, and a sonic nozzle are used to obtain Mach numbers from 0.70 to 1.35. The flow in the test section is stable for approximately 0.5 sec at these Mach numbers. A line drawing of the test section showing model location and a photograph showing the model installed in the test section are presented in Figs. 11 and 12, respectively.

3.4 INSTRUMENTATION AND DATA PRECISION

In Tunnels 4T and 16T all pressures were connected to individual differential pressure transducers. The analog output of the transducers was digitized and fed into a digital computer for calculating local airfoil pressure coefficients.

The estimated precision of measurements is as follows:

α	±0.10 deg
M_∞	±0.003
C_p	±0.02 to ±0.005 for R = 1 to 5 x 10^6, respectively.

In the NASA-HRNT, all pressures were connected to 24-port scanivalves through a fast-acting shutoff valve which trapped a fixed volume

of air between the scanivalve and the shutoff valve. The analog output of the scanivalve differential pressure transducer was digitized and punched on data cards. The data cards were fed into a digital computer for calculating local airfoil pressure coefficients. The pressure range of the scanivalve pressure transducer was changed to measure pressure ranges from 0 to 60, 60 to 200, and 200 to 300 psia. The uncertainty in pressure coefficient is estimated to be ±0.02. Mach number setting in the HRNT is a function of the calibrated tunnel ejector setting, which varies with tunnel blockage ratio. The precision of the Mach number setting was approximately ±0.006 for Mach numbers 0.70 and 0.75 and ±0.010 for Mach numbers 0.80 and 0.85. The variation in centerline Mach number distribution was within ±0.005, based on a tunnel calibration using a centerline static-pressure measuring tube.

SECTION IV
MODEL SUPPORT RIG AND TUNNEL WALL INTERFERENCES

An airfoil section supported by finite end plates allows only a quasi, two-dimensional flow. Although the effects of the finite end plates on the downwash reduce the aspect ratio from an infinite (truly two-dimensional flow) to a finite value, the chordwise loading is essentially independent of spanwise position, and thus the flow over the airfoil is planar. Both visual observations of oil flow and pressure measurements along spanwise locations on the upper surface of the airfoil model indicated that the airflow was planar over the airfoil surface.

An investigation was made during the test of the 24-in.-chord model in Tunnel 16T to determine the blockage effects of the rear part of the support rig which supports the end plates and airfoil section. The fairings (see Fig. 2) were removed from the support cross member and central body to reduce blockage. Data obtained with and without the fairings are compared in Figs. 13 and 14 for Mach numbers 0.80 and 0.85, respectively. The figures indicate that for most flow conditions the differences in data between the normal and small-size support are negligible. However, it should be noted that all subsequent data were obtained with the normal-size support and are under the same effects of support blockage as the data obtained in Tunnel 4T.

To avoid the masking of Reynolds number effects by wall interference, porosity of the test section walls for Tunnel 4T was set based on data obtained with the 6-in.-chord model in Tunnel 16T. The blockage

ratio for the model in Tunnel 16T was 0.043 percent, and the data may be reasonably assumed as near interference-free. The blockage ratio of the model in Tunnel 4T was 0.69 percent. A comparison of Tunnel 4T and 16T data showing the effects of wall porosity is presented in Fig. 15. The pressure coefficients for the upper surface are shown with open symbols, and those for the lower surface are shown with solid symbols. A wall porosity of 6.5 percent was chosen as the best setting for near-interference-free data and was used for all subsequent testing of the airfoil model.

The blockage ratio of the model in the NASA-HRNT was 2.4 percent, and the wall interference was expected to be large. Several calibration runs for various wall porosities were conducted in the NASA-HRNT to match near-interference-free data obtained in Tunnel 16T. Results indicated that the pressure data were insensitive to the wall porosity above 7-percent opening. The data could not be matched to the near-interference-free data by adjusting the wall porosity of the NASA-HRNT. The 7-percent wall porosity was chosen for the whole test program. It should be noted that wall interference is negligible in the NASA tunnel at subcritical flow conditions. Although wall interferences existed at supercritical flow conditions, the data are presented to show trends with Reynolds number variations.

SECTION V
RESULTS AND DISCUSSION

In the present section, the primary considerations are the effects of Reynolds number on free and fixed boundary-layer transition within the region of subcritical and supercritical flow on a quasi, two-dimensional airfoil model.

5.1 REYNOLDS NUMBER EFFECTS

5.1.1 Subcritical Flow

For subcritical flow conditions, the Reynolds number effects are negligible from 6 to 32 million in the NASA-HRNT at M_∞ = 0.7 and 0.75 for free transition and are shown by a single set of data in Figs. 16 and 17, respectively. A similar conclusion may be found from the data obtained in Tunnels 4T and 16T for R_c = 0.3 to 2.6 million and

R_C = 1 to 10 million, respectively. Furthermore, it may be seen in Figs. 16 and 17 that these three sets of data obtained from three different tunnels show good agreement in the different ranges of Reynolds numbers.

The reason for the negligible effects of Reynolds number is that there is no shock wave appearing in the purely subsonic flow field and the phenomena of the shock wave/boundary-layer interaction is absent. Although the characteristics of the boundary layer are changed as the Reynolds number varies, the influence is very limited. The free-transition locations on the model vary with Reynolds number in the different tunnels, which have different tunnel turbulence levels and noise levels. However, the effect is restricted to skin friction in the attached flow with corresponding negligible effects on the pressure distribution on the airfoil. Hence, it is reasonable to assume that scaling effects in the subcritical, attached-flow regime are negligible.

5.1.2 Supercritical Flow

For supercritical flow conditions, attached flow and flow with rear (trailing edge) separation were typical. The shock wave interaction with the laminar as compared to the turbulent boundary layer gives a completely different shock wave pattern and pressure distribution on the airfoil (Ref. 9). In the laminar interaction, two or more upstream-inclined shock waves appear, as shown in the sketch below. The local flow is reduced from supersonic to subsonic velocity as it crosses the most rearward shock of the series of shock waves. The location of this rearward shock is selected as representative of the main flow feature. This corresponds to the single, nearly normal or downstream-inclined shock wave in the turbulent interaction case. In both cases, a large pressure gradient occurs in the neighborhood of the shock wave. This steep pressure change is the primary cause of local and rear separations. The lifting- and pitching-moment coefficients of the airfoil depend on the location of the shock wave. Hence, the shock wave location will be used to examine the effects of Reynolds number in the later sections.

The pressure distributions on the airfoil for supercritical flow at M_∞ = 0.8 are shown in Fig. 18 for various angles of attack. Data obtained from Tunnel 4T and NASA-HRNT on the 6-in. airfoil and from Tunnel 16T on the 24-in. airfoil cover the Reynolds number range from 0.3 to 41.7 million. The pressure data at M_∞ = 0.8 indicate no rear separation for angles of attack of -2, 0, or 2 deg. The movement

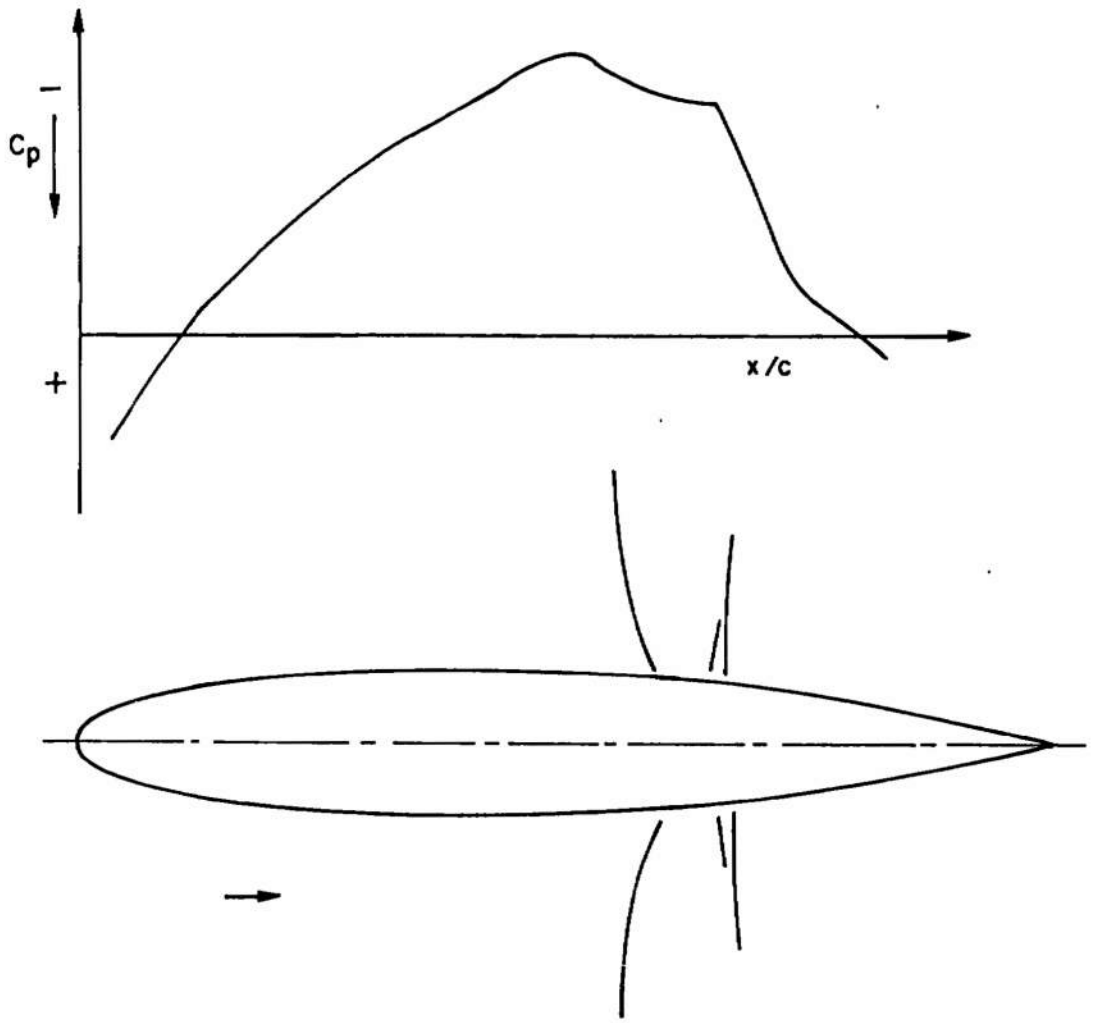

Surface Pressure Distribution and Shock Wave Pattern in Laminar Boundary-Layer Interaction

of the shock wave on the upper surface with the variation in Reynolds number is within 10 percent of the airfoil chord length.

For the higher chord Reynolds numbers, the pressure distributions indicate that boundary-layer separation occurred aft of the airfoil shock location for angles of attack of 5.3 deg on the 6-in.-chord model in Tunnel 4T and 4 deg on the 24-in.-chord model in Tunnel 16T. This phenomenon is associated with the difference in tunnel transition Reynolds number characteristics, which will be explained in a later section of this report.

For laminar interaction, the negative peak pressure is not as high as that for the turbulent case. Two or more shock waves in the flow make the surface pressure change gradually, except at the neighborhood of the rearward shock, which has a large pressure gradient. As Reynolds number increases, the transition point moves upstream of the shock wave, and the turbulent interaction with the familiar steep pressure increase becomes predominant.

The effects of Reynolds number on the shock wave location are summarized in Fig. 19. The shock wave moves forward with increasing Reynolds number for the laminar interaction conditions. This is evident in Fig. 19 for R_c = 0.3 to 2.0 million. When the turbulent interaction occurs, the shock wave moves rearward with increasing Reynolds number greater than R_c = 2.0 million for -2 deg $\leq \alpha \leq$ 2 deg. Data from the NASA-HRNT at zero angle of attack indicate the slow trend of the shock wave movement toward the trailing edge with increasing Reynolds numbers above about 6 million.

The disparity between data obtained in Tunnel 16T with the 24-in.-chord model and that obtained in Tunnel 4T with the 6-in.-chord model could be the effect of the differences in transition Reynolds number characteristics of the two tunnels. A transition Reynolds number investigation (Ref. 11) was conducted in the two tunnels using a 10-deg cone model. The results of that investigation indicated that Tunnel 4T had a lower transition Reynolds number for the lower unit Reynolds numbers and approached that of Tunnel 16T as unit Reynolds number was increased. This would indicate that the data obtained in Tunnel 4T are in reality for boundary-layer transition locations of higher effective chord Reynolds number conditions. Shifting the Tunnel 4T data in Fig. 19 to higher chord Reynolds numbers would result in closer agreement with the Tunnel 16T data.

5.1.3 Supercritical Flow with Rear Separation

Rear separation is indicated by an insufficient pressure recovery at the upper-surface trailing edge of the airfoil. As shown in Fig. 20 for M_∞ = 0.85, rear separation exists for most higher Reynolds numbers at angles of attack of 2 deg and greater. The movement of the shock wave on the upper surface under these conditions has a range of 15 percent of the chord length. This large movement of the shock wave contrasts with the attached flow at M_∞ = 0.8 and is attributed to the rear separation of the boundary layer.

The effects of Reynolds number on the shock wave location for the M_∞ = 0.85 case are summarized in Fig. 21. The trends are similar to those obtained at M_∞ = 0.8. In the case of laminar interaction, the shock wave moves forward as Reynolds number increases from R_c = 0.3 to 1.6 million. After the turbulent interaction appears, the shock wave moves rearward slowly with increasing Reynolds number up to R_c = 30 million.

The disparity between the data of Tunnels 16T and 4T at the same chord Reynolds number for M_∞ = 0.85 is more pronounced than that for M_∞ = 0.8. As mentioned before, the two tunnels have different transition Reynolds number characteristics, and hence the characteristics of the boundary layer at the shock wave are different. Also, the degree of rear separation is different for the two tunnels. For example, the rear separation in Tunnel 4T for $R_c = 2.6 \times 10^6$ is more severe than that in 16T, as shown in Figs. 20c and d.

5.2 TRANSITION STRIP EFFECTS

The pressure data presented in the previous paragraphs were obtained for the natural-transition condition. The natural-transition location is determined by the tunnel noise, the tunnel turbulence level, and the unit Reynolds number. Data discussed here were obtained for various fixed-transition strips. The width of the strips was 1/8 in. for both the 6-in. and the 24-in. airfoils. The sizes of the carborundum transition strips chosen based on Ref. 10 criteria were Grit No. 120 and Grit No. 80 for the 6-in. and 24-in. airfoils, respectively. The strips change the characteristics of the boundary layer and hence the interaction pattern with the shock wave. The gross effects of the transition strip on the pressure distribution will be discussed below for the upper surface only.

5.2.1 Subcritical Flow for Fixed Transition

As indicated previously, the subcritical flow pattern is insensitive to the characteristics of the boundary layer and hence to the variation of Reynolds number. Similarly, the effects of transition location are also negligible since the transition strip is only a mechanism to fix the transition location artifically and to change the characteristics of the boundary layer.

5.2.2 Supercritical Flow For Fixed Transition

Data on the 6-in. airfoil were obtained with the transition strips fixed at 17.5-, 32.5-, and 47.5-percent chord positions. Data on the 24-in. airfoil were obtained with the transition strip fixed at the 17.5-percent chord location only.

The pressure data at $M_\infty = 0.8$ shown in Fig. 22b were obtained at various fixed-transition locations in the range of Reynolds numbers between 0.3 and 10.2 million. In Tunnel 4T, all of the fixed-transition cases were tripped into a turbulent boundary layer upstream of the shock wave except for $R_c = 0.3$ and 0.5 million, where the laminar boundary layer is too thick to be tripped effectively by the strip. Similarly, data obtained in Tunnel 16T on the 24-in. airfoil at $R_c = 1 \times 10^6$ indicate that the boundary layer remained laminar downstream to the shock wave location.

The movement in shock wave location with variations in Reynolds number for a given fixed transition exhibits a trend similar to that of natural transition, as shown in Fig. 23. The shock wave moves forward for R_c less than 2×10^6 but moves rearward slightly for R_c greater than 2×10^6 for angles of attack of less than 2 deg. The limited data for $\alpha = 4$ and 5.3 deg also exhibit this trend.

The pressure distributions on the upper surface at $M_\infty = 0.85$ shown in Fig. 24 are for various fixed-transition locations in the range of Reynolds numbers between 0.3 and 10.2 million. In several cases such as $R_c = 1.0 \times 10^6$ in Tunnel 16T, the boundary layer remains laminar at the foot of the shock wave due to the ineffectiveness of the transition strips. For all instances of shock wave/turbulent boundary-layer interaction, the trailing-edge pressure exhibits good recovery with little or no indication of trailing-edge separation. The variations in shock wave location for different Reynolds numbers are shown in Fig. 25. The general trend is similar to that for $M_\infty = 0.8$.

5.3 HIGH REYNOLDS NUMBER SIMULATION

The aerodynamic phenomena of the shock wave/boundary-layer interaction on the C-141 airfoil have been discussed in the preceding paragraphs. Specifically mentioned have been scaling effects of Reynolds number and effects of transition strips. The complete simulation of all details of the flow field is not possible, since the characteristics

of boundary-layer growth depend on unit Reynolds number. However, satisfactory equivalence in the overall effects producing the same net results given by the fixed-transition strips was achieved for the present test of the C-141 airfoil, and this demonstrates the feasibility of using low Reynolds number tests in existing tunnels for high Reynolds number simulation on this type of airfoil.

The variation in shock wave location on the quasi, two-dimensional C-141 airfoil is limited to the range of 15-percent chord, as shown in Figs. 19 and 21. The fixed-transition strips are able to trip the boundary layer into a turbulent boundary layer upstream of the shock location and sustain a positive pressure recovery aft of the shock location. Two flow conditions given below demonstrate the simulation. For $M_\infty = 0.8$, $\alpha = 0$, the shock wave location at high Reynolds number (near 40 million) may be duplicated on the 6-in. model with a transition strip at the 17.5-percent chord location and an R_c of about 1×10^6. For $M_\infty = 0.85$, $\alpha = 0$, duplication with fixed transition at the 32.5-percent chord location and an R_c of about 0.6×10^6 is possible.

The flow pattern and surface pressure depend largely upon the characteristics of the boundary layer in the neighborhood of the shock wave and at the trailing edge. Also, the rear separation dominates the shock wave location and, consequently, the pressure distribution over all the airfoil. Hence, the simulation of the flow field should attempt to match both the trailing-edge condition and the shock wave location for high Reynolds number.

SECTION VI
CONCLUDING REMARKS

The pressure distributions on the 6- and 24-in.-chord models of the C-141 airfoil were obtained in the range of Reynolds numbers from 0.3 to 41 million at Mach numbers 0.7, 0.75, 0.8, and 0.85 and at angles of attack of $\alpha = -2$, 0, 2, 4, and 5.3 deg. Two typical flows existed on the model: the subcritical flow, which had no local supersonic Mach number, and the supercritical flow, which had a supersonic flow region embedded in a subsonic flow field. The subcritical flow was insensitive to Reynolds number variations, indicating little or no scaling effects. The effects of fixed transition on the pressure distribution in the subcritical flow also were negligible.

For the supercritical flow condition, the pronounced differences in the shock wave pattern and surface pressure depended upon whether the boundary layer was laminar or turbulent at the shock location. The difference of the shock wave location is very pronounced between the separated and attached flows at the trailing edge.

For the smooth configuration, the natural transition point, which is determined by the tunnel flow quality (i. e., noise, turbulence level, and unit Reynolds number), is equally as important a factor for the flow field as is the chord Reynolds number. In order to match the flow field, both transition location and chord Reynolds number should be matched simultaneously for different models in different tunnels.

The effectiveness of a grit-type transition strip in fixing transition point depends on the size of grit, tunnel unit Reynolds number, and the location of the grit with respect to the leading edge. Although a guideline in the selection of grit is available in the literature, a choice of transition location is not yet predictable. A systematic study seems necessary for the determination of transition location by artifically fixing transition.

The details of the flow characteristics cannot be expected to match completely for subscale simulation. Furthermore, the results of this study on the C-141 airfoil indicate that the high Reynolds number (10^7) tests are not necessarily better than the low Reynolds number tests unless they are close to the full-scale flight value. Nevertheless, the approximate gross effects can be simulated. The procedure for scaling high Reynolds number data is proposed as follows:

1. Obtain sample data for the airfoil using existing low-productive, high Reynolds number test facilities.

2. Compare the sample data to previously established data for airfoils with a similar class pressure distribution (e.g., a roof-type or peaky-type pressure distribution) and determine whether the scaling technique used during that test is applicable or

3. Using the sample data as a master, test the model in a high-productive, low Reynolds number test facility, and establish the simplest means of adjusting shock location through boundary-layer transition adjustment.

The simplest method available to modify the boundary layer is that using the grit-type boundary-layer trip, which worked well on the C-141 airfoil. There are several other techniques available, such as vortex generator, model cooling, and powered boundary-layer control systems - blowing or suction slots. It is recommended that the simplest means of modifying the boundary layer be taken first and then some other boundary-layer control device used to adjust the flow until the flow field is simulated.

Another approach would be to calculate the airfoil flight Reynolds number characteristics such as shock wave location, surface pressure distribution, normal-force and pitching-moment coefficients, and boundary-layer characteristics. Some means are required to adjust shock location through boundary-layer control devices to modify the flow until the flow field is simulated as predicted. The complexity of work involved with this approach makes it apparent that a detailed study for predicting airfoil surface pressure distributions, including viscous effects, is urgently needed.

REFERENCES

1. Pearcey, H. H., Osborne, J., and Haines, A. B. "The Interactions Between Local Effects at the Shock and Rear Separation - a Source of Significant Scale Effects in Wind Tunnel Tests on Airfoils and Wings." Article in "Transonic Aerodynamics," AGARD CP 35, September 1968.

2. Osborne, J. and Pearcey, H. H. "A Type of Stall with Leading-Edge Transonic Flow and Rear Separation." Article in "Facilities and Techniques for Aerodynamic Testing at Transonic Speeds and High Reynolds Number." AGARD CP 83, April 1971.

3. Loving, D. L. "Wind-Tunnel-Flight Correlation of Shock-Induced Separated Flow." NASA TN D-3580, September 1966.

4. Stanewsky, E. and Little, B. H. "Studies of Separation and Reattachment in Transonic Flow." AIAA Paper 70-541, 1970.

5. Harper, C. W. "Prospects in Aeronautics Research and Development." J. Aircraft, Vol. 5, No. 5 (September-October, 1968), pp. 417-426.

6. Blackwell, J. A. "Preliminary Study of Effects of Reynolds Number and Boundary-Layer Transition Location on Shock-Induced Separation." NASA TND-5003, January 1969.

7. Groeneweg, J. I. "Some Remarks on the Applicability of Shifting Boundary-Layer Transition to Reduce Scale Effects at Transonic Speeds." AC-69-29, National Aerospace Laboratory NLR, the Netherlands.

8. Test Facilities Handbook (Ninth Edition). "Propulsion Wind Tunnel Facilities, Vol. 4." Arnold Engineering Development Center, July 1971.

9. Liepmann, H. W. "The Interaction Between Boundary Layer and Shock Waves in Transonic Flow." J. Aeron. Sci., Vol. 13, No. 12 (December 1946), pp. 623-637.

10. Braslow, A. L., Hicks, R. M., and Harris, R. V. "Use of Grit-Type Boundary-Layer-Transition Trips on Wind-Tunnel Models." NASA TN D-3579, September 1966.

11. Credle, O. P. and Carleton, W. E. "Determination of Transition Reynolds Number in the Transonic Mach Number Range." AEDC-TR-70-218 (AD875995), October 1970.

APPENDIXES

I. ILLUSTRATIONS

II. TABLE

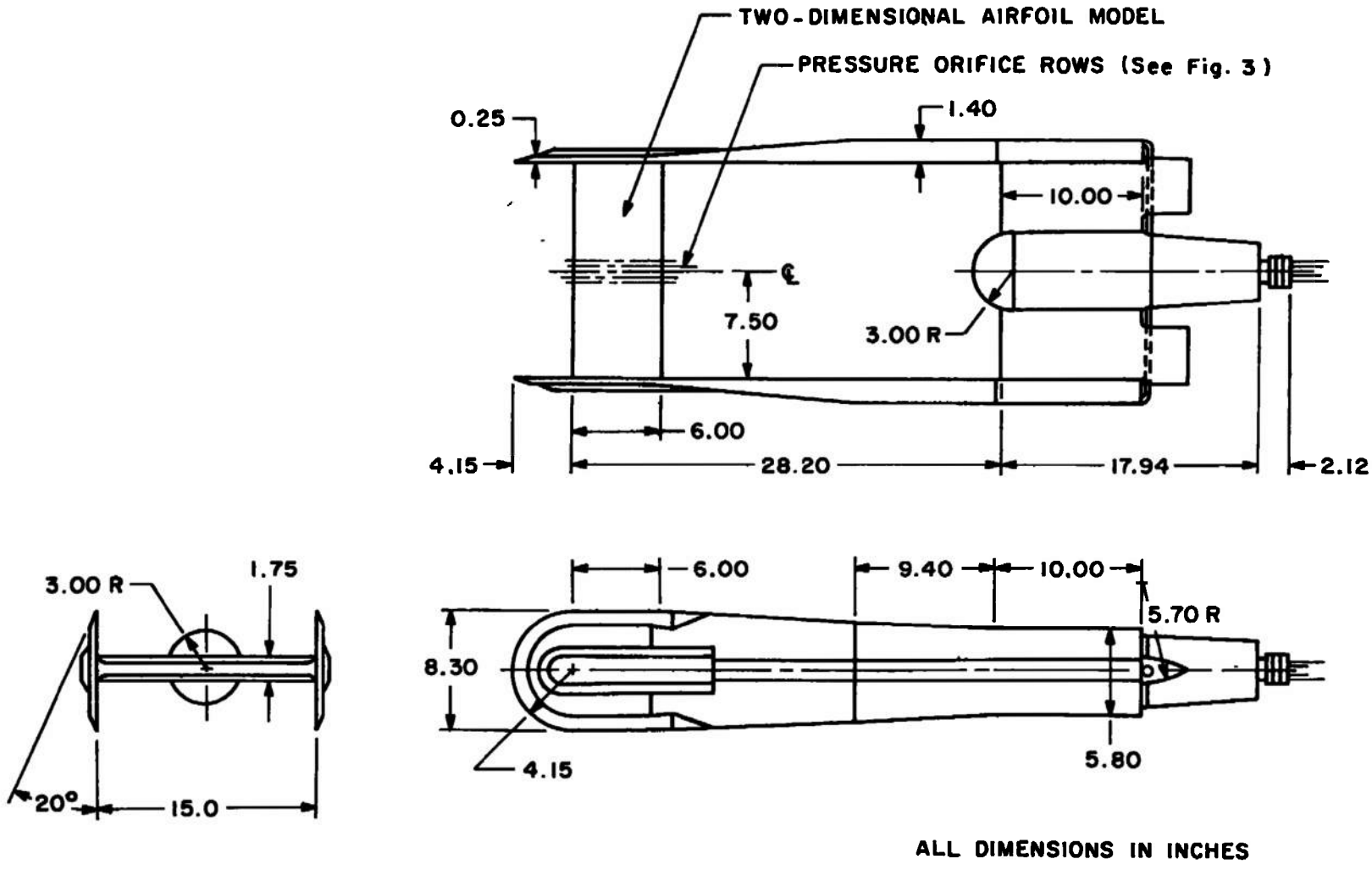

Fig. 1 Details of 6-in.-Chord Airfoil Model Support Hardware

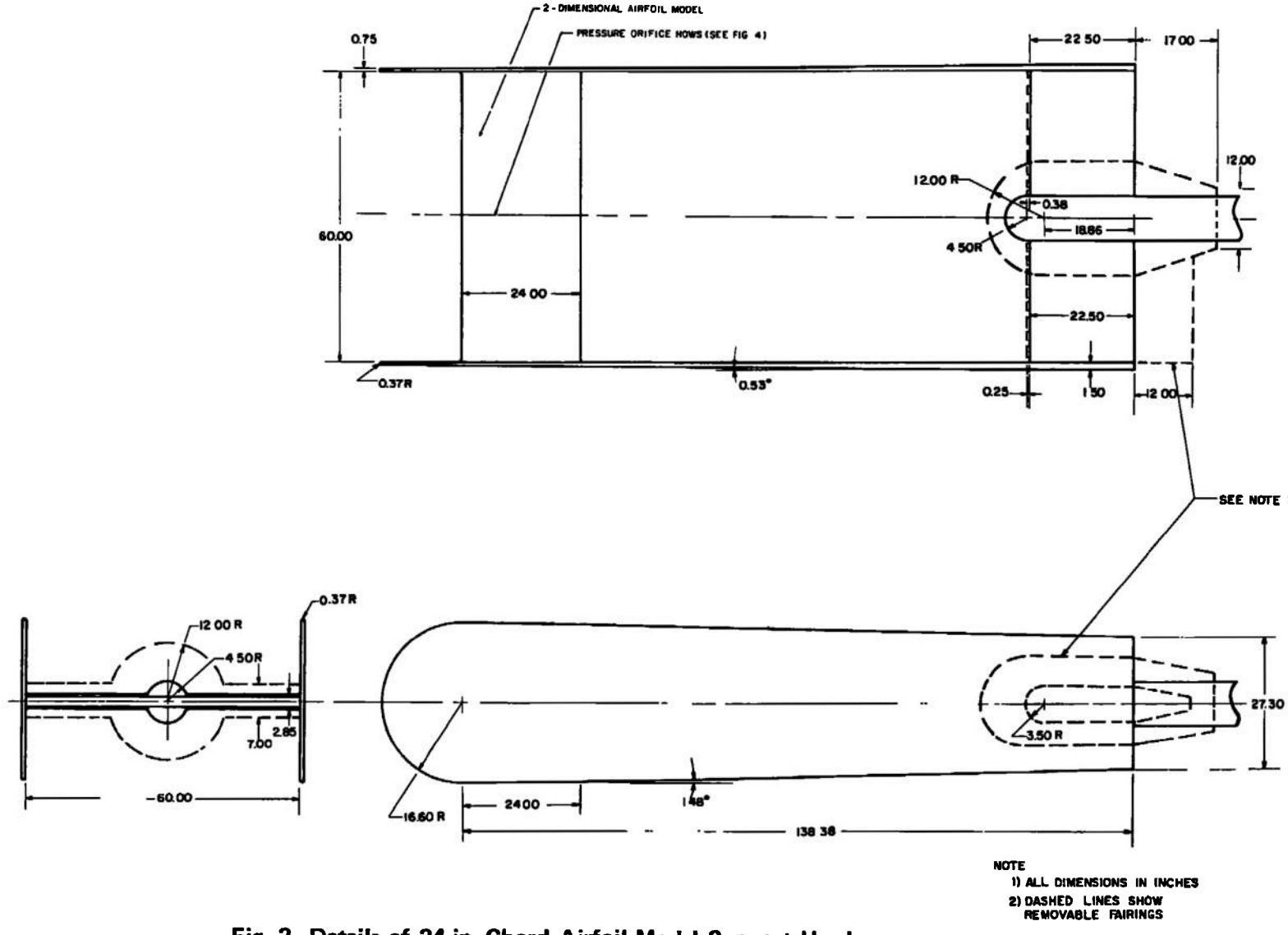

Fig. 2 Details of 24-in.-Chord Airfoil Model Support Hardware

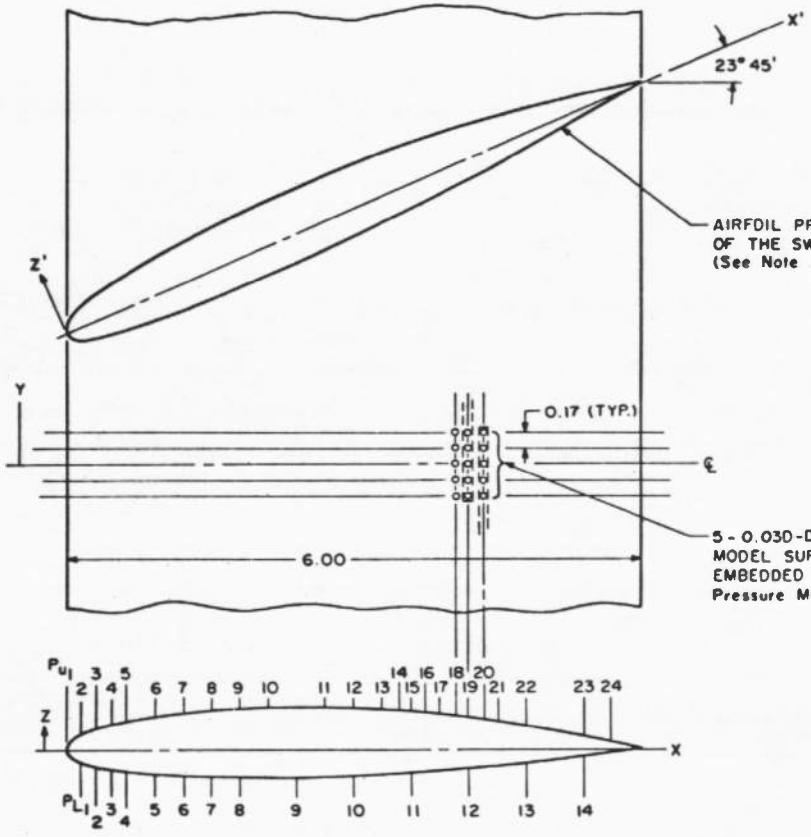

6-IN. CHORD		
X/C	P_U	P_L
0.000	1	
0.025	2	1
0.050	3	2
0.075	4	3
0.100	5	4
0.150	6	5
0.200	7	6
0.250	8	7
0.300	9	8
0.350	10	
0.400		9
0.450	11	
0.500	12	10
0.550	13	
0.580	14	
0.600	15	11
0.625	16	
0.650	17	
0.680	18	
0.700	19	12
0.730	20	
0.750	21	
0.800	22	13
0.900	23	14
0.945	24	

NOTE: 1. ALL DIMENSIONS IN INCHES
2. DIMENSIONS X FOR THE AIRFOIL MODEL ARE 0.9153 OF THE SWEPT DIMENSION X', Z AND Z' DIMENSIONS ARE IDENTICAL.

Fig. 3 Pressure Orifice Location and Airfoil Simulation Details on 6-in.-Chord Airfoil Model

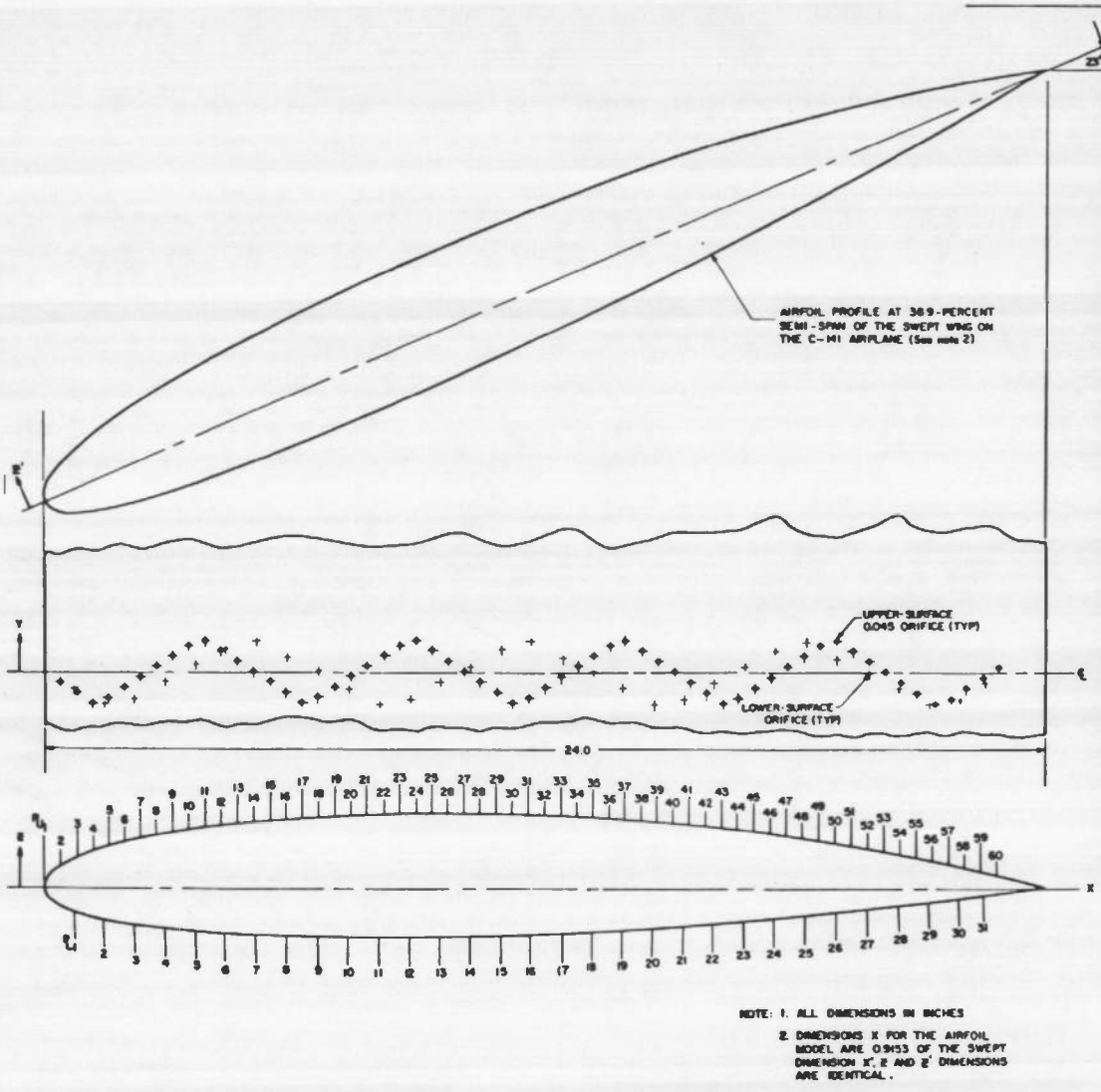

24-IN CHORD							
$X_{/C}$	$Y_{/C}$	P_U	P_L	$X_{/C}$	$Y_{/C}$	P_U	P_L
0.0000	0.0000	1		0.5760	0.0312	37	
0.0160	-0.0104	2		0.5779	-0.0156		19
0.0304	-0.0156		1	0.5920	0.0208	38	
0.0320	-0.0208	3		0.6080	0.0104	39	
0.0480	-0.0312	4		0.6083	-0.0312		20
0.0608	-0.0312		2	0.6240	0.0000	40	
0.0640	-0.0260	5		0.6387	-0.0234		21
0.0800	-0.0156	6		0.6400	0.0104	41	
0.0912	-0.0234		3	0.6560	-0.0208	42	
0.0960	-0.0052	7		0.6692	-0.0078		22
0.1120	0.0052	8		0.6720	-0.0312	43	
0.1217	-0.0078		4	0.6880	-0.0260	44	
0.1280	0.0156	9		0.6996	0.0078		23
0.1440	0.0260	10		0.7040	-0.0156	45	
0.1521	0.0078		5	0.7200	-0.0052	46	
0.1600	0.0312	11		0.7300	0.0234		24
0.1780	0.0208	12		0.7360	0.0052	47	
0.1825	0.0234		6	0.7520	0.0156	48	
0.1920	0.0104	13		0.7604	0.0312		25
0.2080	0.0000	14		0.7680	0.0260	49	
0.2129	0.0312		7	0.7840	0.0313	50	
0.2240	-0.0104	15		0.7871	0.0156		26
0.2400	-0.0208	16		0.8000	0.0208	51	
0.2433	0.0156		8	0.8160	0.0104	52	
0.2560	-0.0312	17		0.8212	0.0000		27
0.2720	-0.0260	18		0.8320	0.0000	53	
0.2736	0.0000		9	0.8480	-0.0104	54	
0.2880	-0.0156	19		0.8517	-0.0146		28
0.3040	-0.0052	20		0.8640	-0.0208	55	
0.3047	-0.0156		10	0.8800	-0.0313	56	
0.3200	0.0052	21		0.8821	0.0312		29
0.3346	-0.0312		11	0.8960	-0.0260	57	
0.3360	0.0156	22		0.9120	-0.0156	58	
0.3520	0.0260	23		0.9125	-0.0234		30
0.3650	-0.0234		12	0.9280	-0.0052	59	
0.3680	0.0312	24		0.9377	-0.0078		31
0.3840	0.0208	25		0.9440	0.0052	60	
0.3954	-0.0078		13	0.9010	1.1250	61	
0.4000	0.0104	26			0.6250	62	
0.4160	0.0000	27			0.1250	63	
0.4258	0.0078		14		0.1250	64	
0.4320	-0.0104	28			0.3750	65	
0.4480	-0.0208	29			0.6250	66	
0.4562	0.0234		15		0.8750	67	
0.4640	-0.0312	30			1.1250	68	
0.4800	-0.0260	31		0.7200	1.1250	69	
0.4867	0.0312		16		0.6250	70	
0.4960	-0.0156	32			0.1250	71	
0.5120	-0.0052	33			0.1250	72	
0.5171	0.0156		17		0.3750	73	
0.5280	0.0052	34			0.6250	74	
0.5440	0.0156	35			0.8750	75	
0.5475	0.0000		18		1.1250	76	
0.5600	0.0260	36					

NOTE: 1. ALL DIMENSIONS IN INCHES

2. DIMENSIONS X FOR THE AIRFOIL MODEL ARE 0.9953 OF THE SWEPT DIMENSION X', Z AND Z' DIMENSIONS ARE IDENTICAL.

Fig. 4 Pressure Orifice Location and Airfoil Simulation Details on 24-in.-Chord Airfoil Model

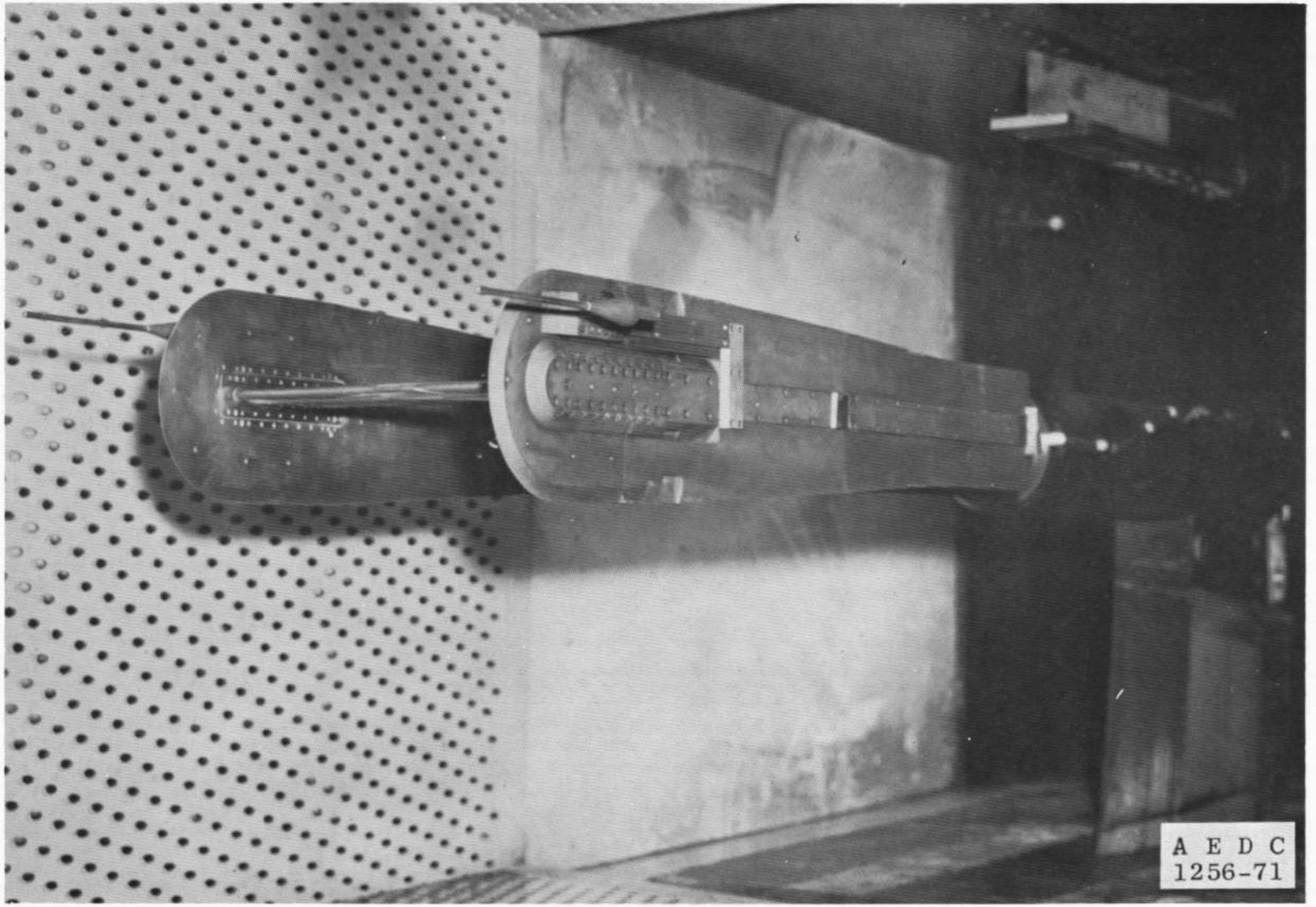

Fig. 5 Photograph of 6-in.-Chord Airfoil Model Installed in Tunnel 4T Test Section

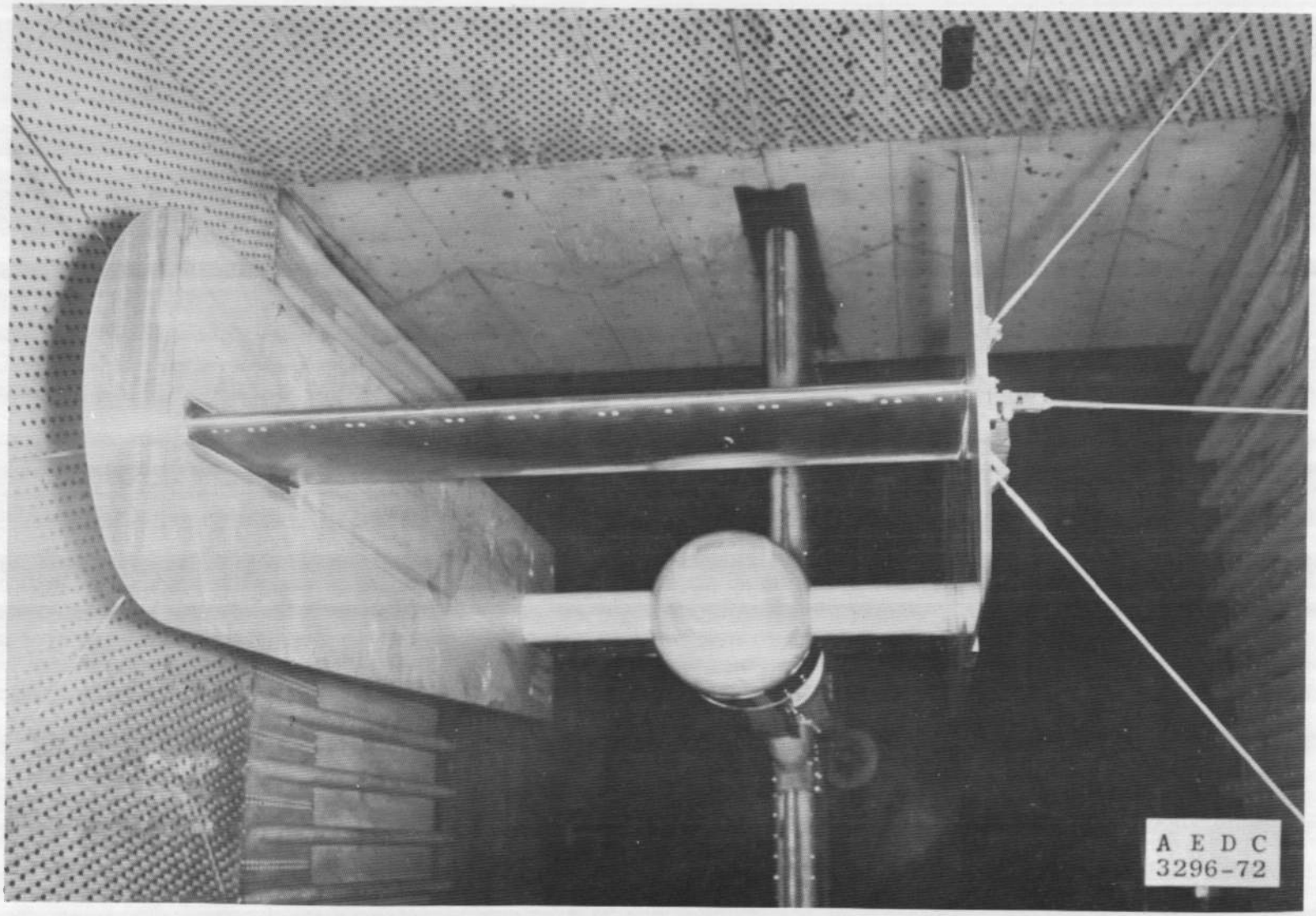

Fig. 6 Photograph of 24-in.-Chord Airfoil Model Installed in Tunnel 16T Test Section

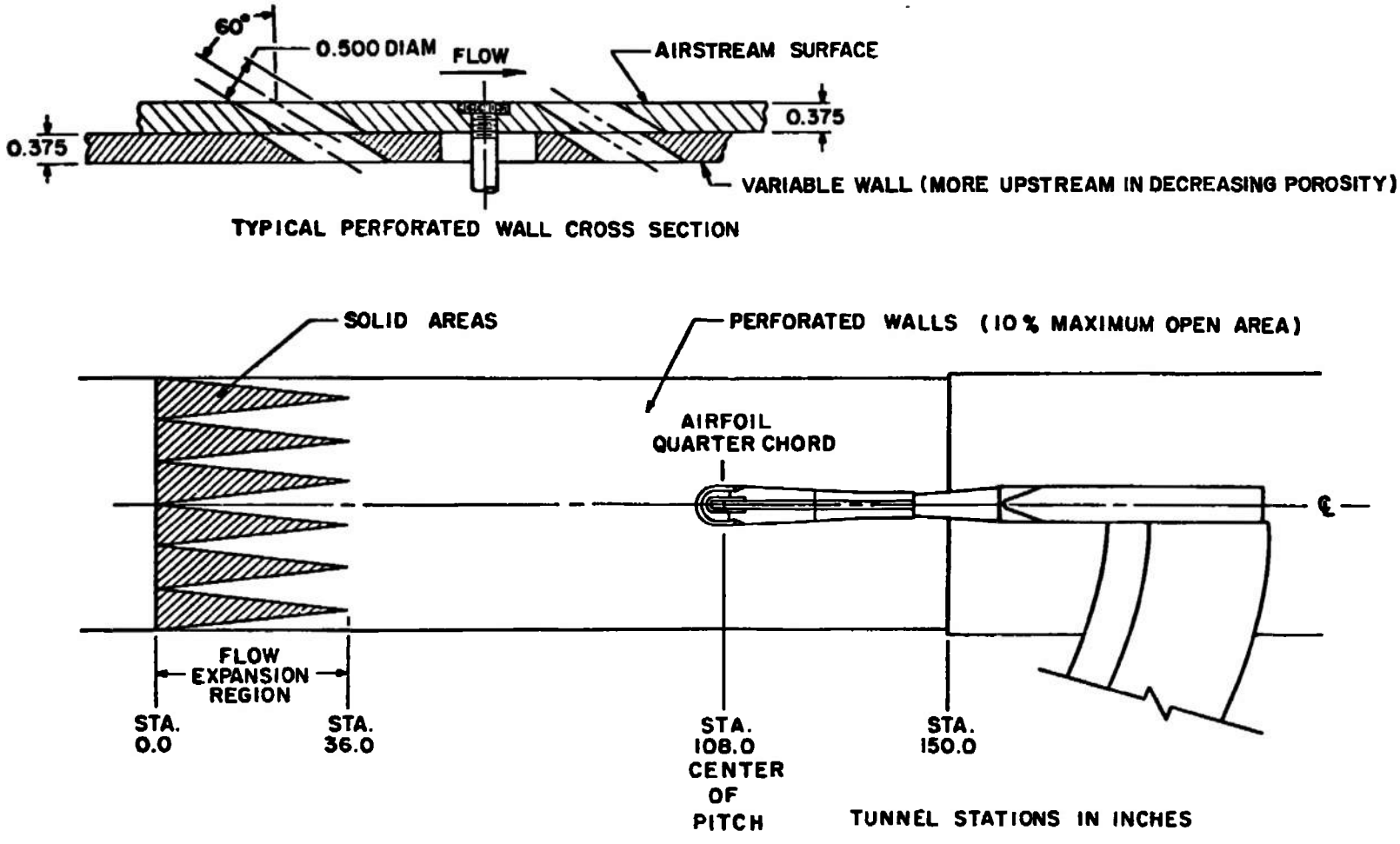

Fig. 7 Tunnel 4T Test Section Showing 6-in.-Chord Airfoil Model Location

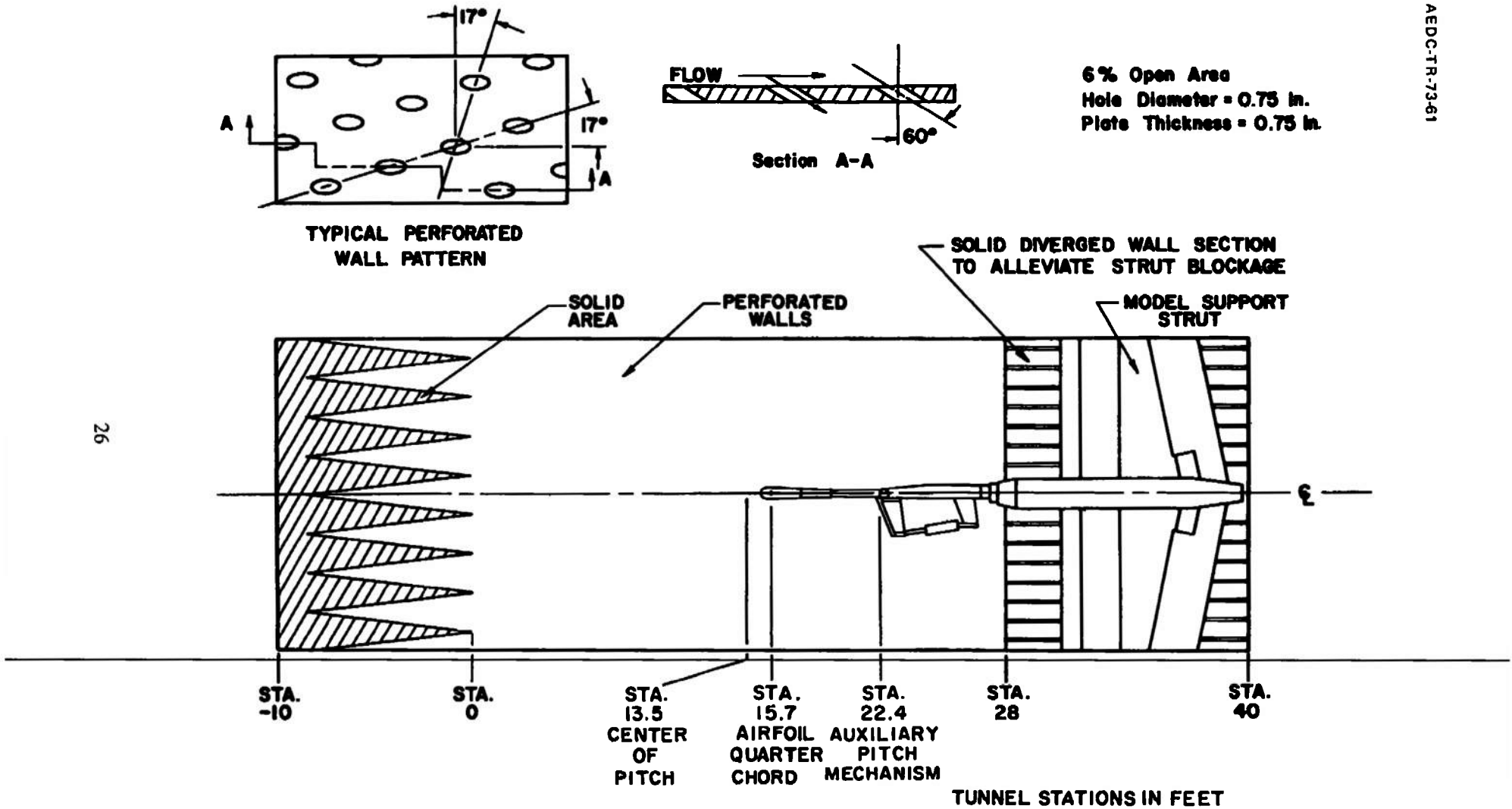

Fig. 8 Tunnel 16T Test Section Showing 6-in.-Chord Airfoil Model Location

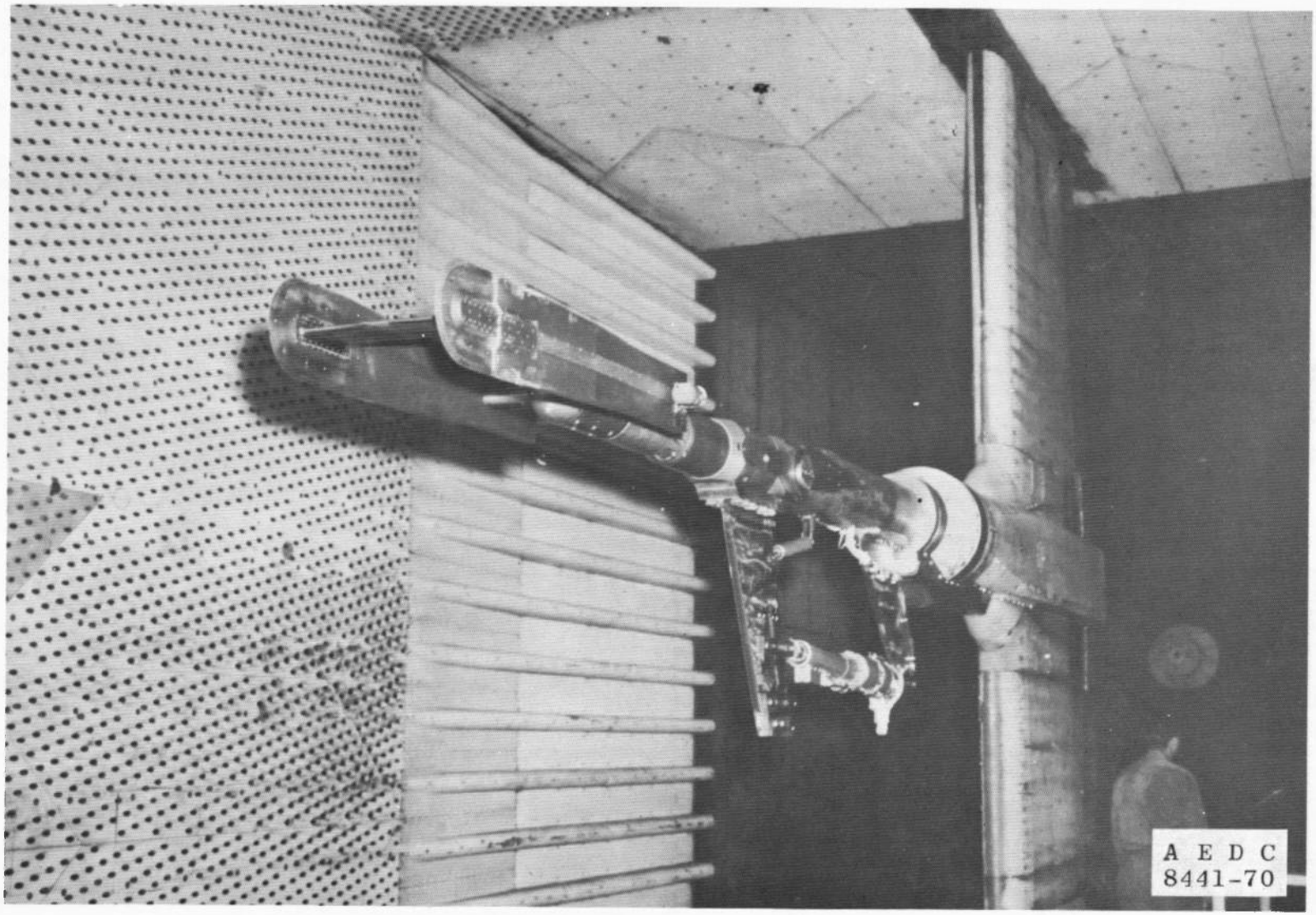

Fig. 9 Photograph of 6-in.-Chord Airfoil Model Installed in Tunnel 16T Test Section

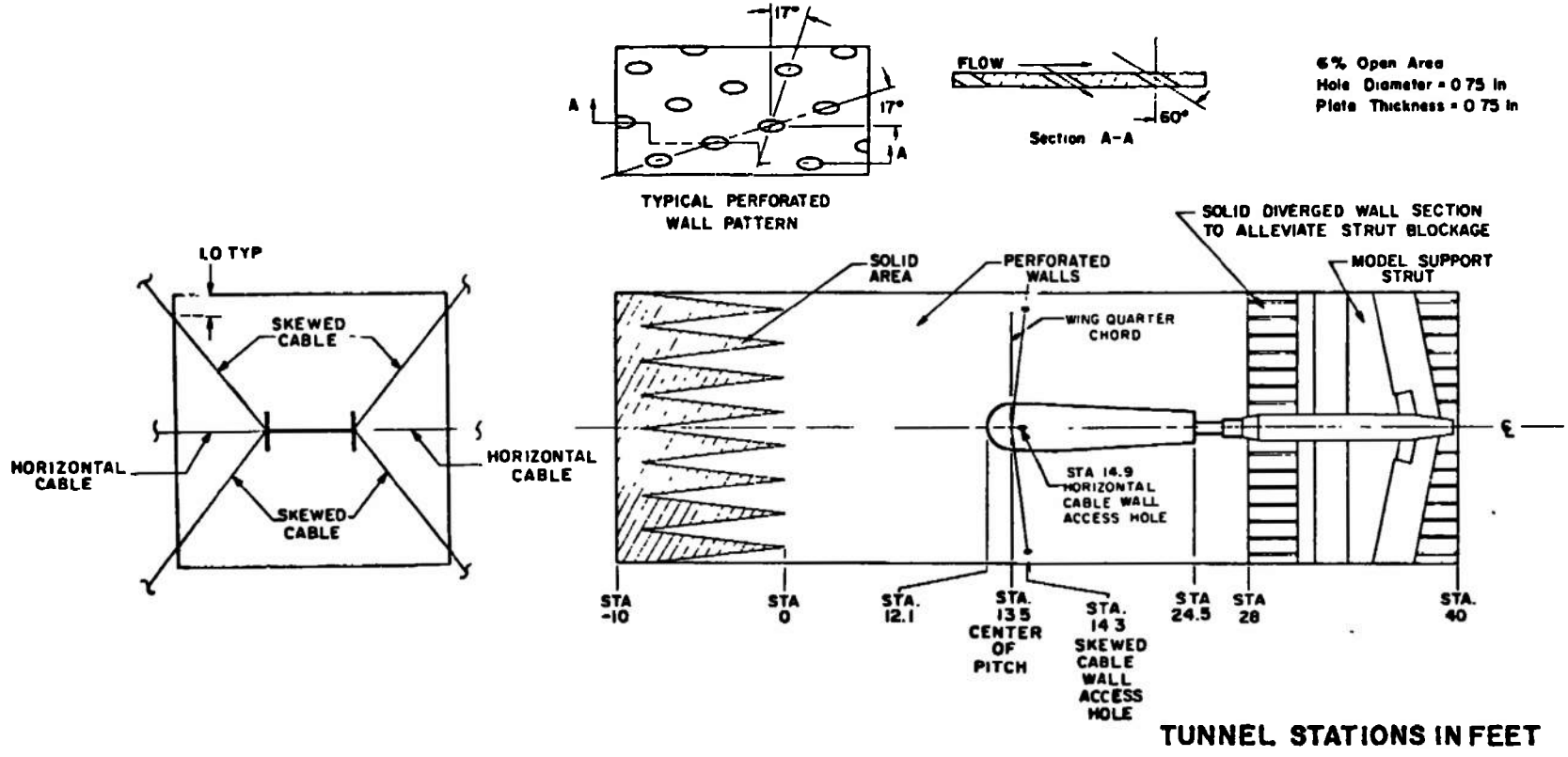

Fig. 10 Tunnel 16T Test Section Showing 24-in.-Chord Airfoil Model Location

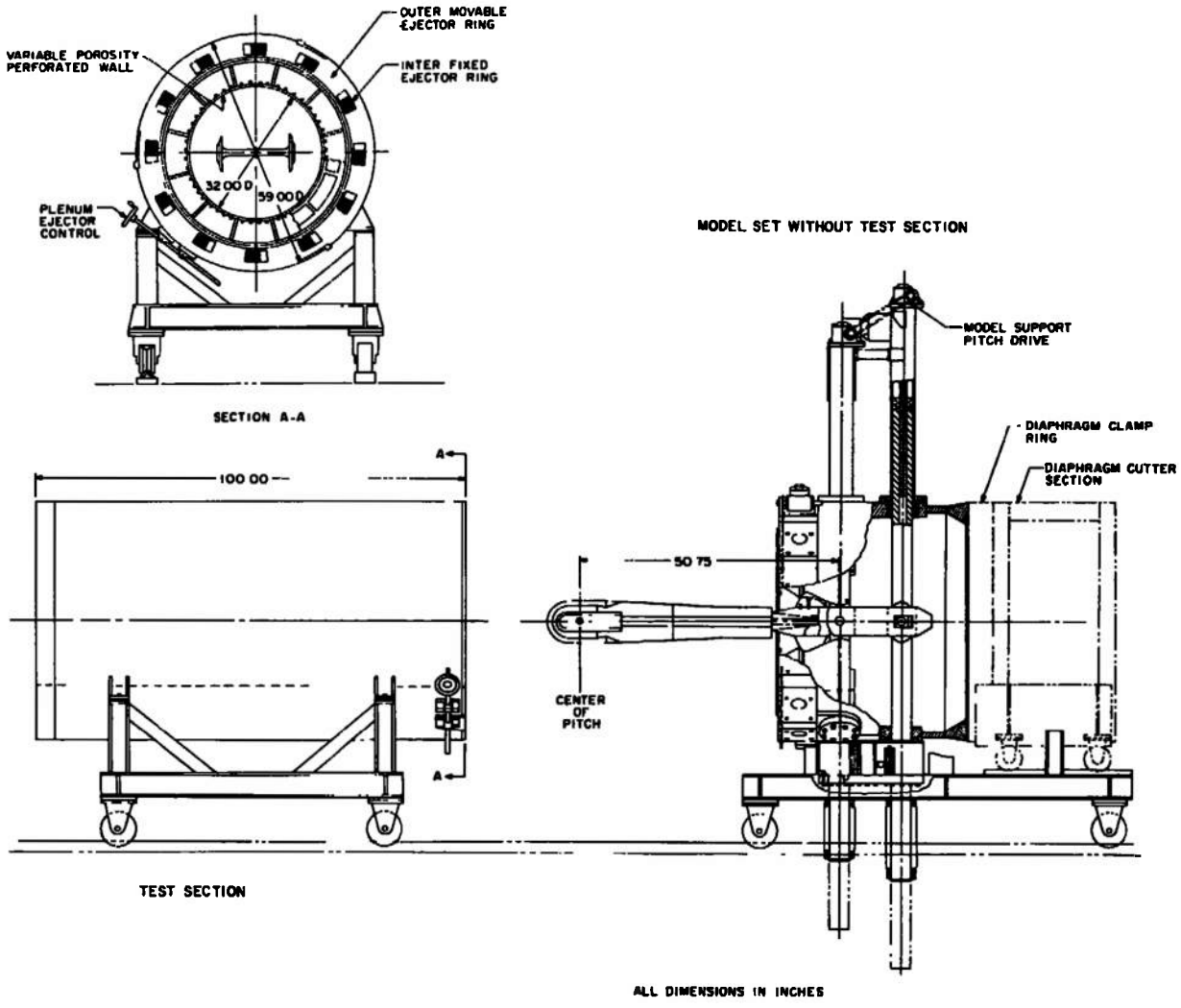

Fig. 11 Test Section of Marshall Space Flight Center High Reynolds Number Tunnel Showing 6-in.-Chord Airfoil Model Location

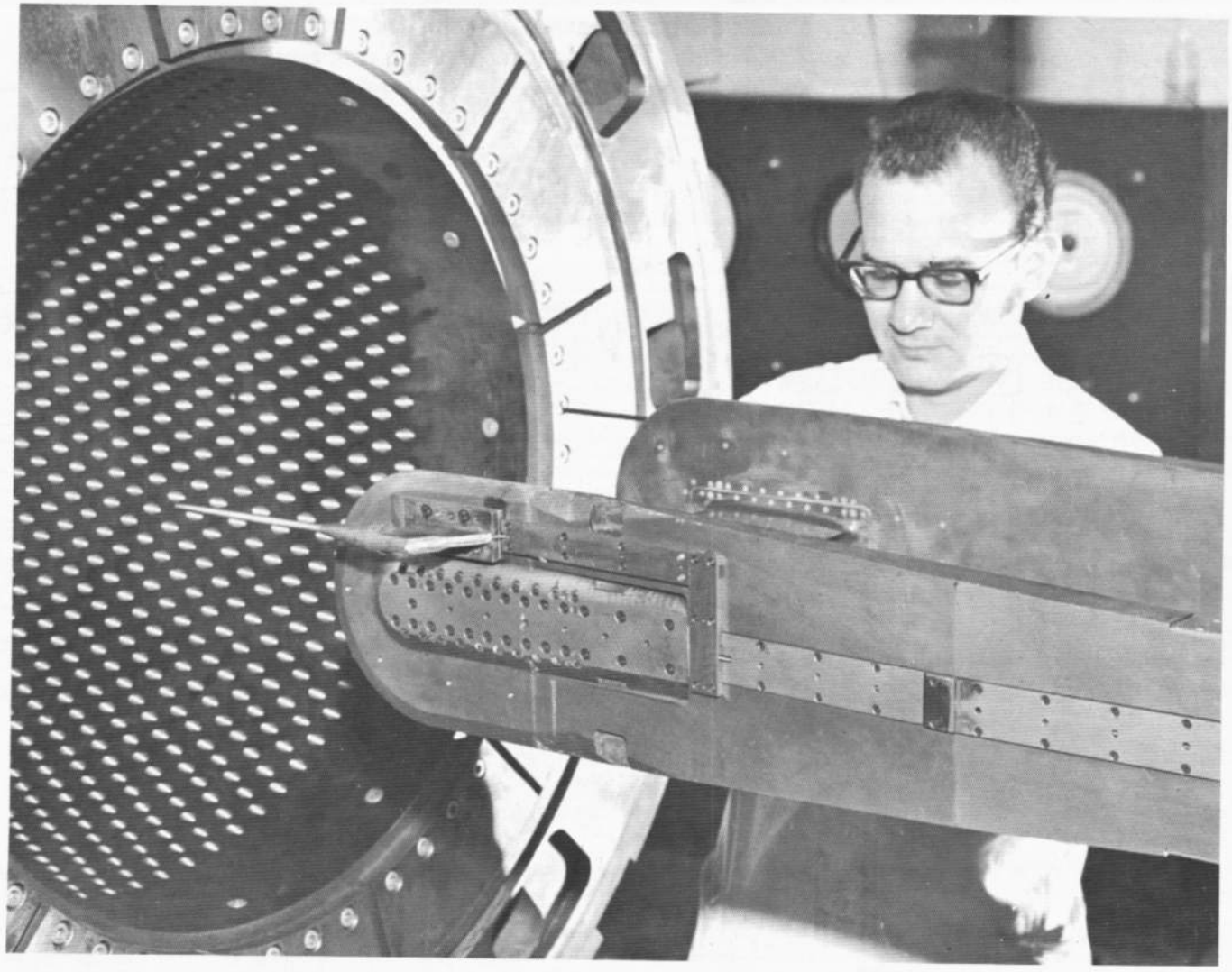

Fig. 12 Photograph of 6-in.-Chord Airfoil Model Installation in Marshall Space Flight Center High Reynolds Number Tunnel

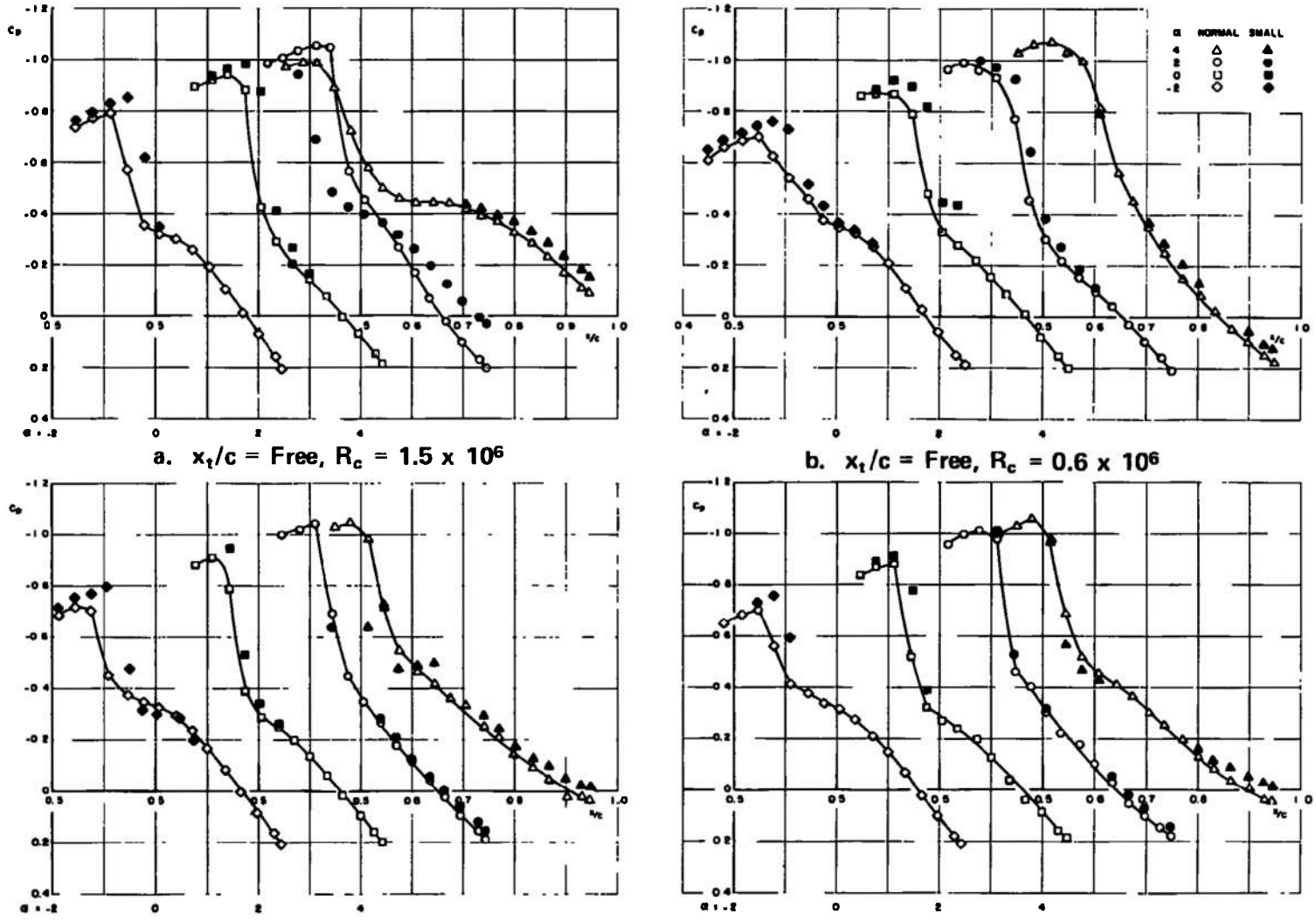

a. x_t/c = Free, R_c = 1.5 x 10^6

b. x_t/c = Free, R_c = 0.6 x 10^6

c. x_t/c = 17.5 percent, R_c = 2.5 x 10^6

d. x_t/c = 17.5 percent, R_c = 1.5 x 10^6

Fig. 13 Effect of Support Blockage on the Upper-Surface Pressure Distribution of the 24-in.-Chord Airfoil Model in Tunnel 16T at M_∞ = 0.80 and α = -2 to 4 deg

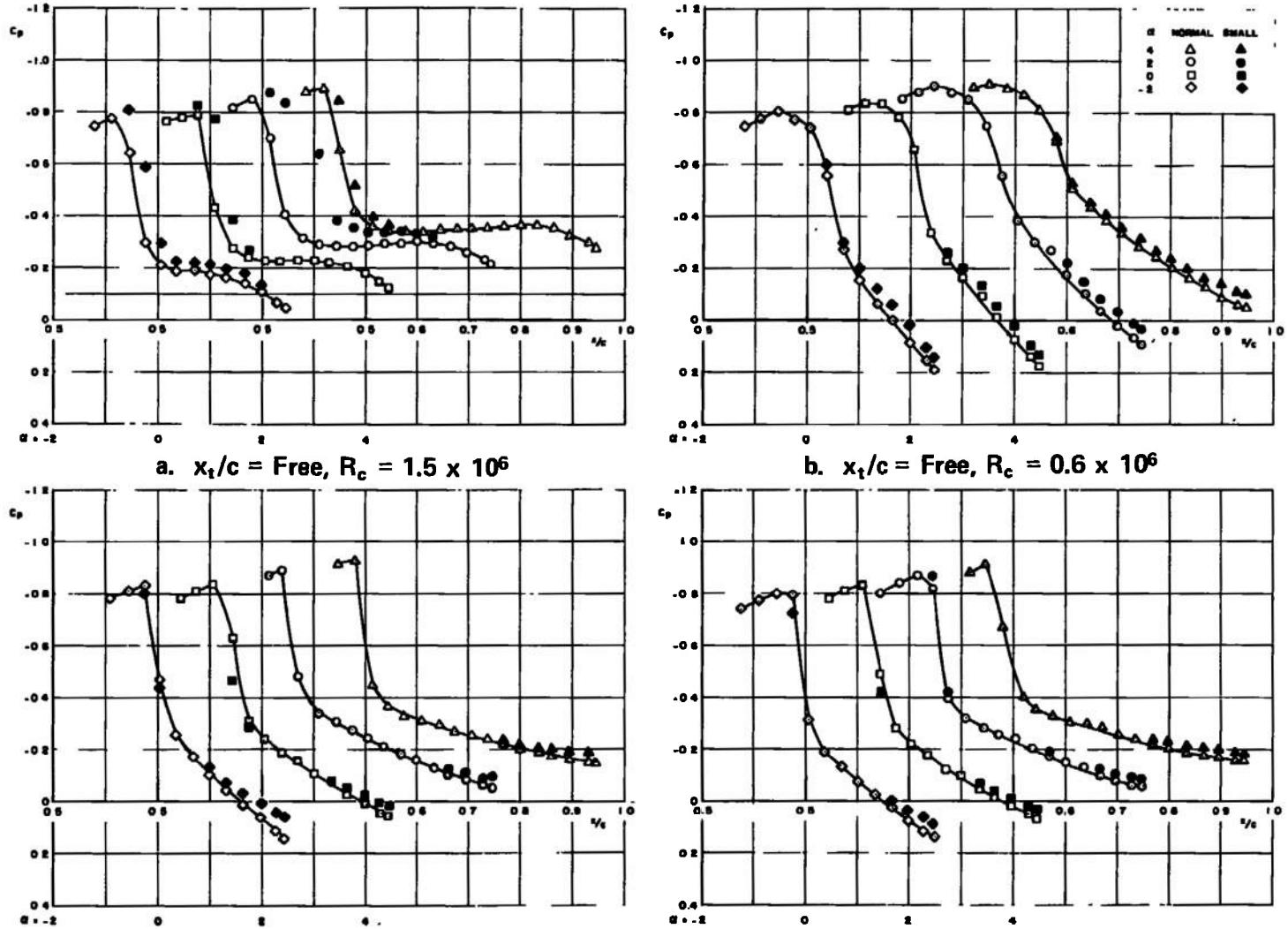

a. x_t/c = Free, $R_c = 1.5 \times 10^6$

b. x_t/c = Free, $R_c = 0.6 \times 10^6$

c. x_t/c = 17.5 percent, $R_c = 2.5 \times 10^6$

d. x_t/c = 17.5 percent, $R_c = 1.5 \times 10^6$

Fig. 14 Effect of Support Blockage on the Upper-Surface Pressure Distribution of the 24-in.-Chord Airfoil Model in Tunnel 16T at $M_\infty = 0.85$ and α = -2 to 4 deg

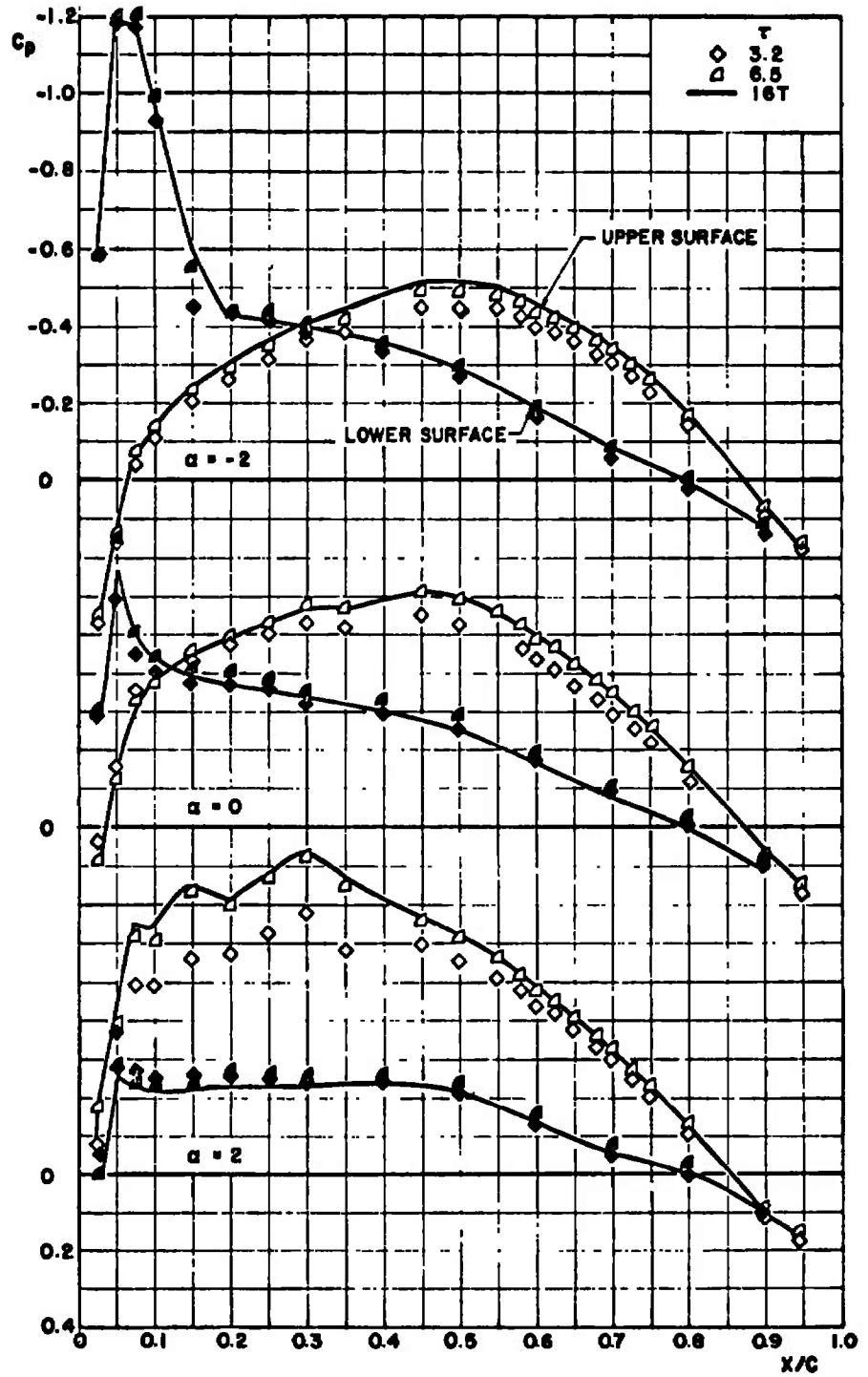

a. $M_\infty = 0.75$

Fig. 15 Effect of Tunnel 4T Test Section Wall Porosity on the Surface Pressure Distribution of the 6-in.-Chord Airfoil Model for x_t/c = Free and $R_c = 2.5 \times 10^6$, α = -2, 0, and 2 deg

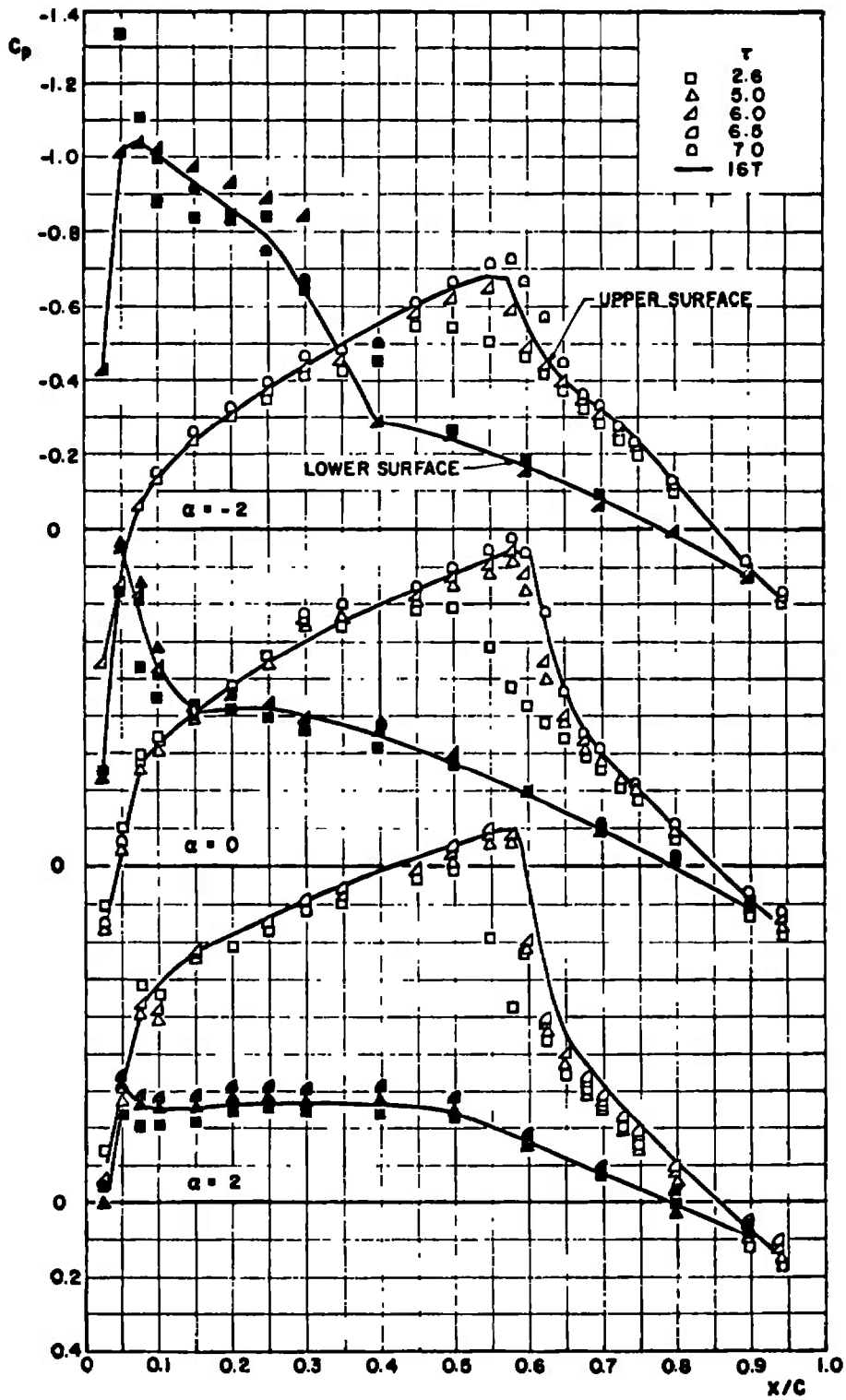

b. $M_\infty = 0.80$

Fig. 15 Continued

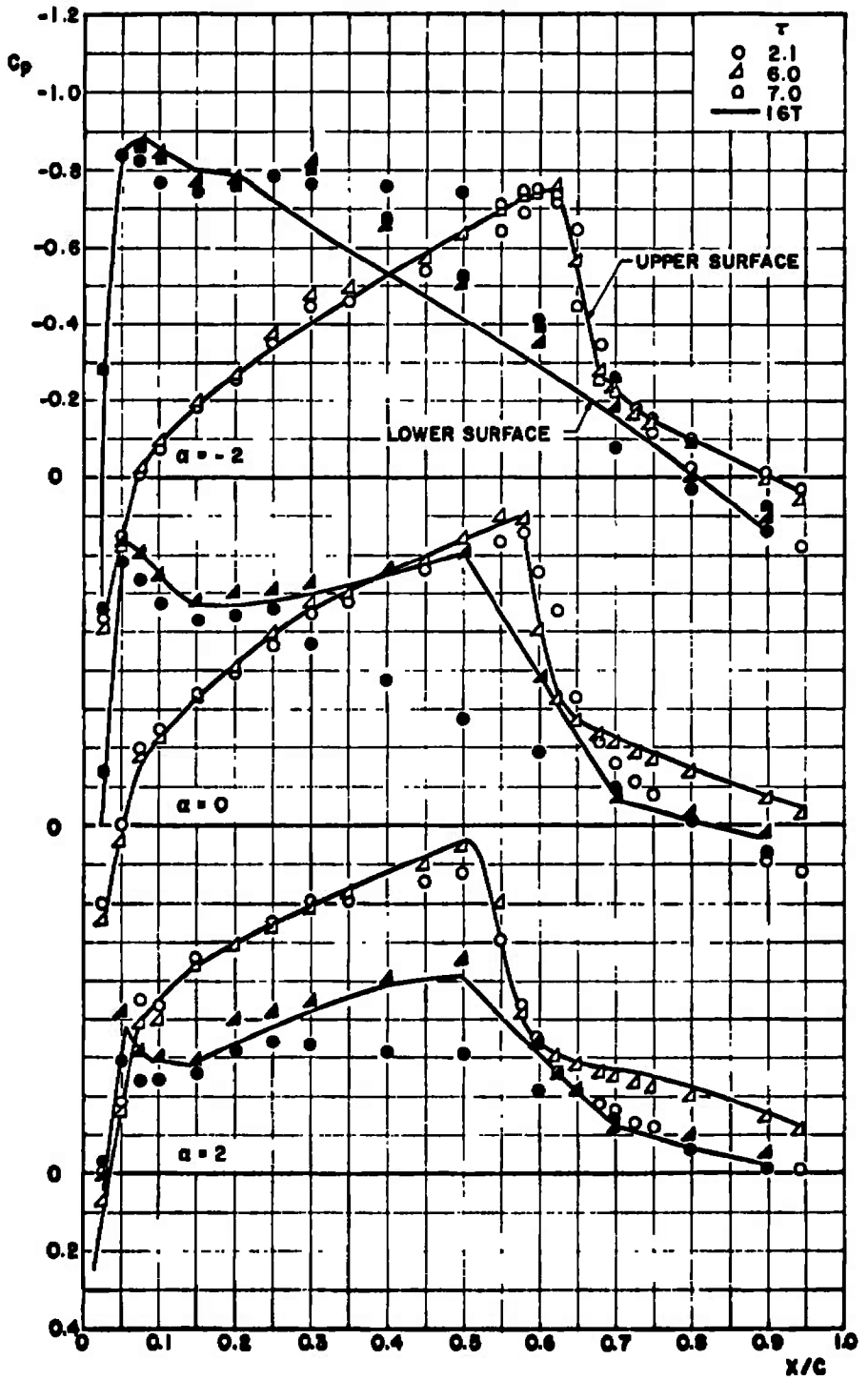

c. $M_\infty = 0.85$

Fig. 15 Concluded

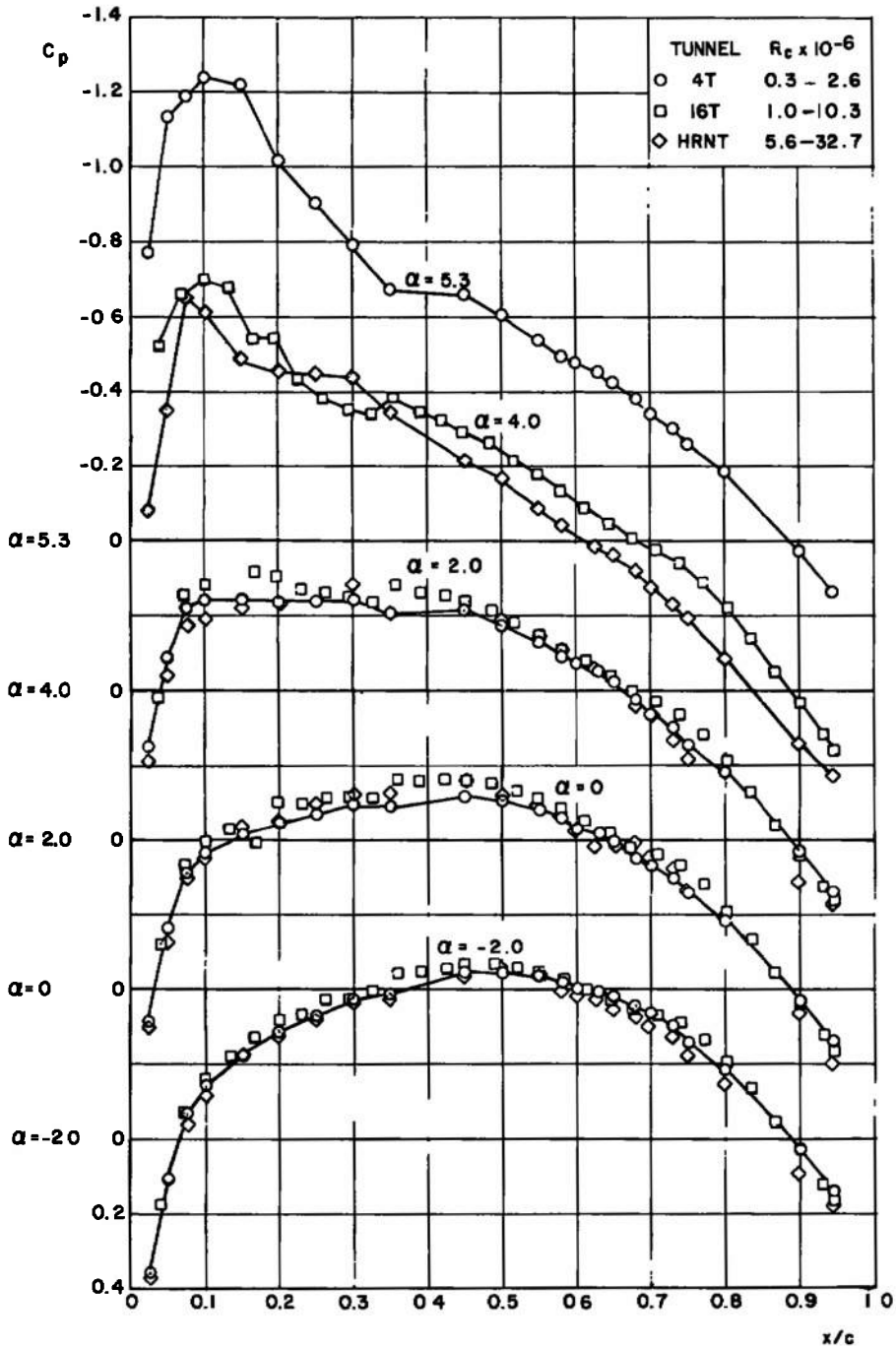

a. Upper Surface

Fig. 16 Typical Pressure Distribution on the Airfoil Models in All Tunnels for All Variations in x_t/c and R_c at $M_\infty = 0.70$ and α = -2 to 5.25 deg

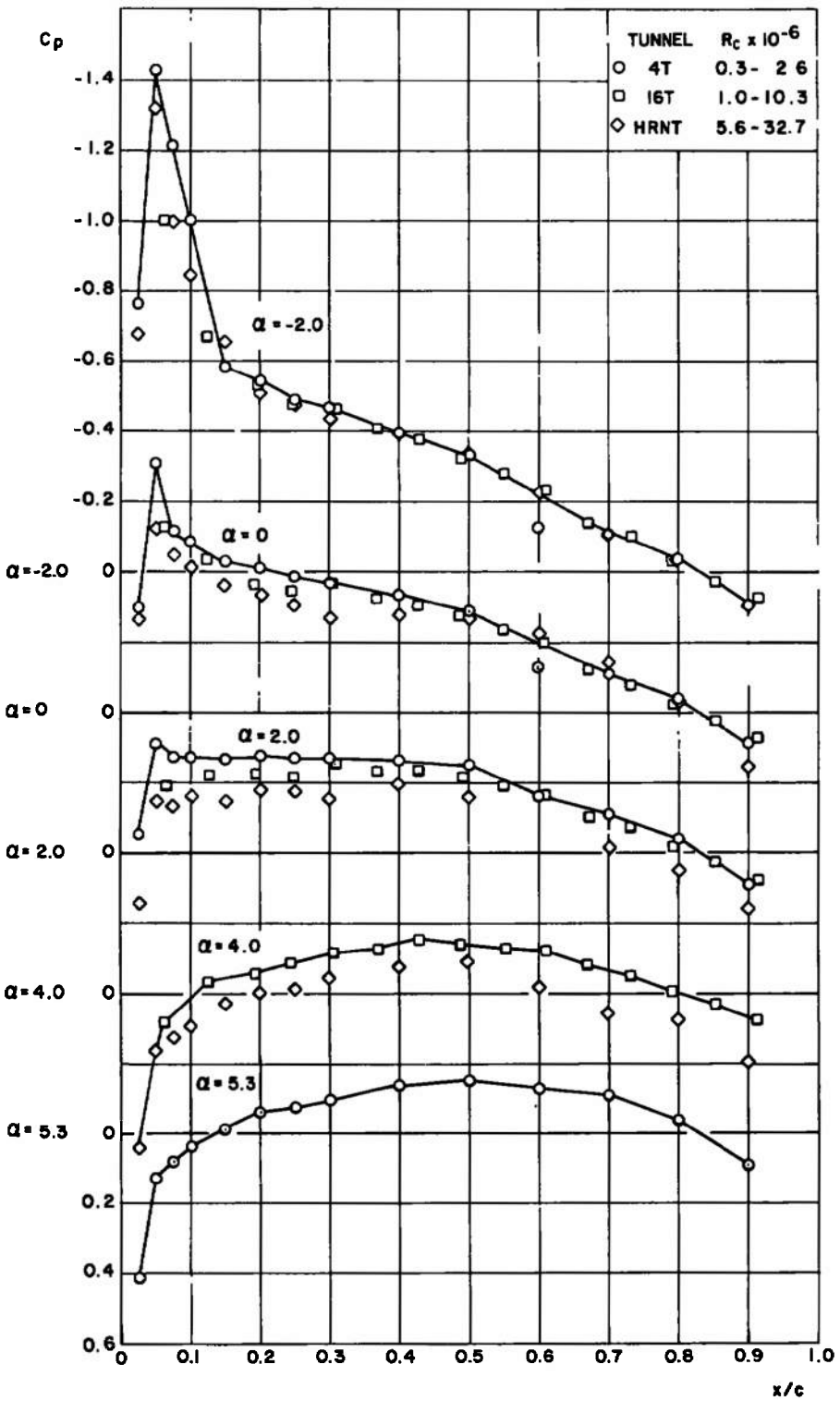

b. Lower Surface

Fig. 16 Concluded

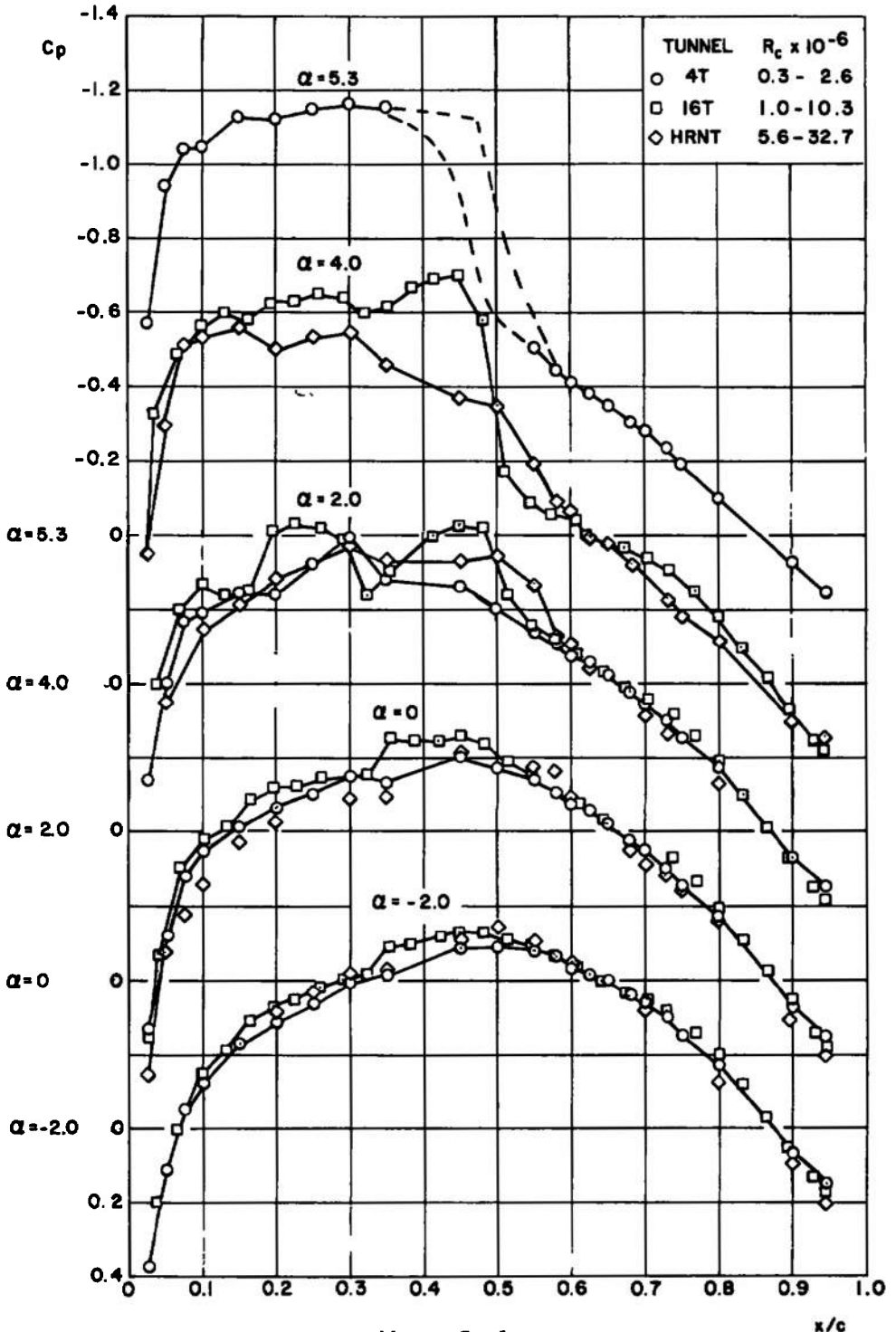

a. Upper Surface

Fig. 17 Typical Pressure Distribution on the Airfoil Models in All Tunnels for All Variations in x_t/c and R_c at $M_\infty = 0.75$ and $\alpha = -2$ to 5.25 deg

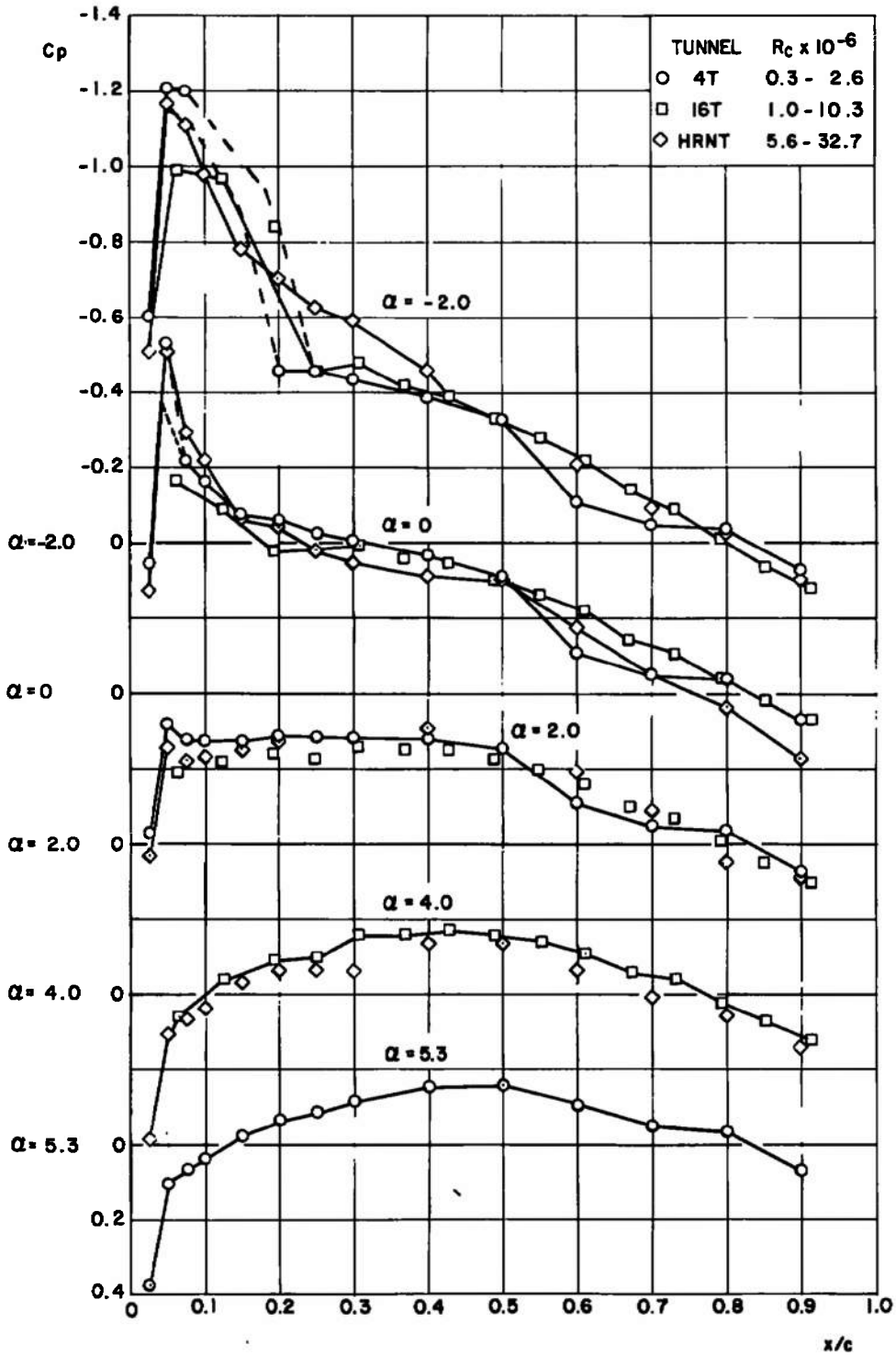

b. Lower Surface
Fig. 17 Concluded

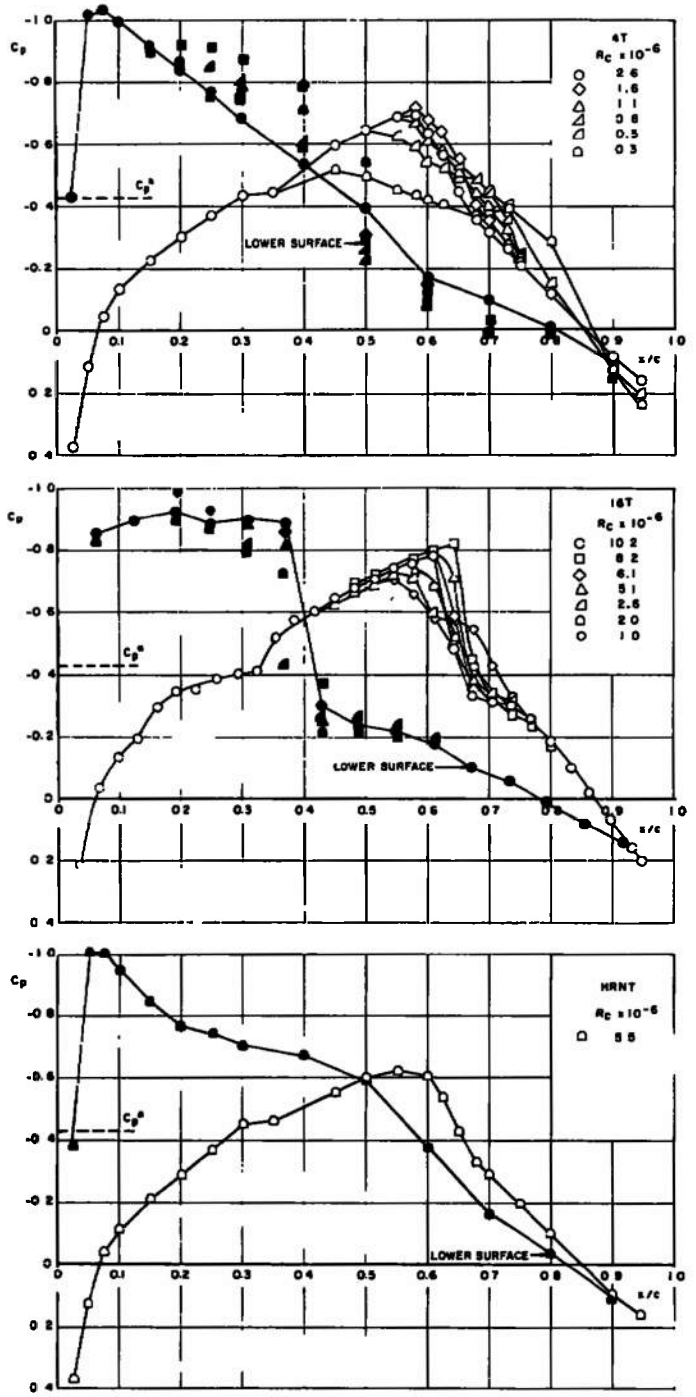

a. α = -2 deg

Fig. 18 Effect of Reynolds Number on the Pressure Distribution of the Airfoil Models in Various Tunnels at M_∞ = 0.8

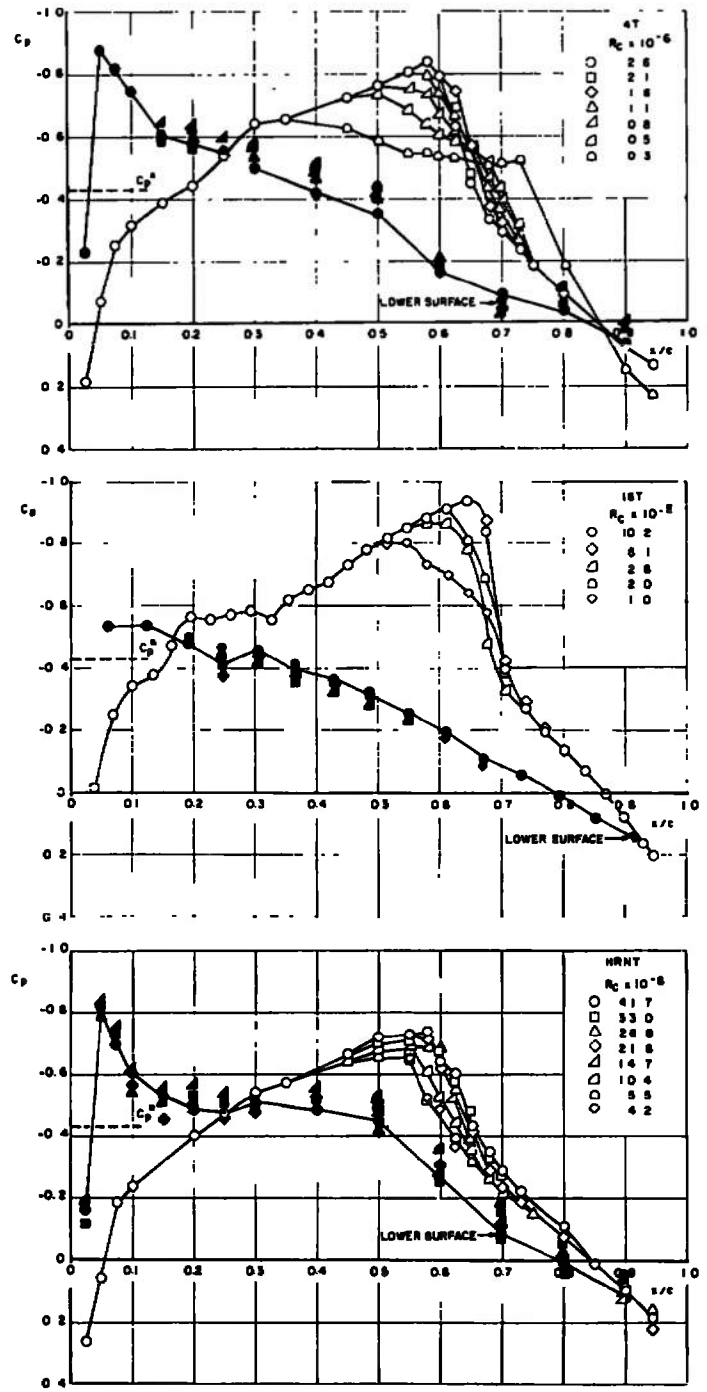

b. α = 0 deg
Fig. 18 Continued

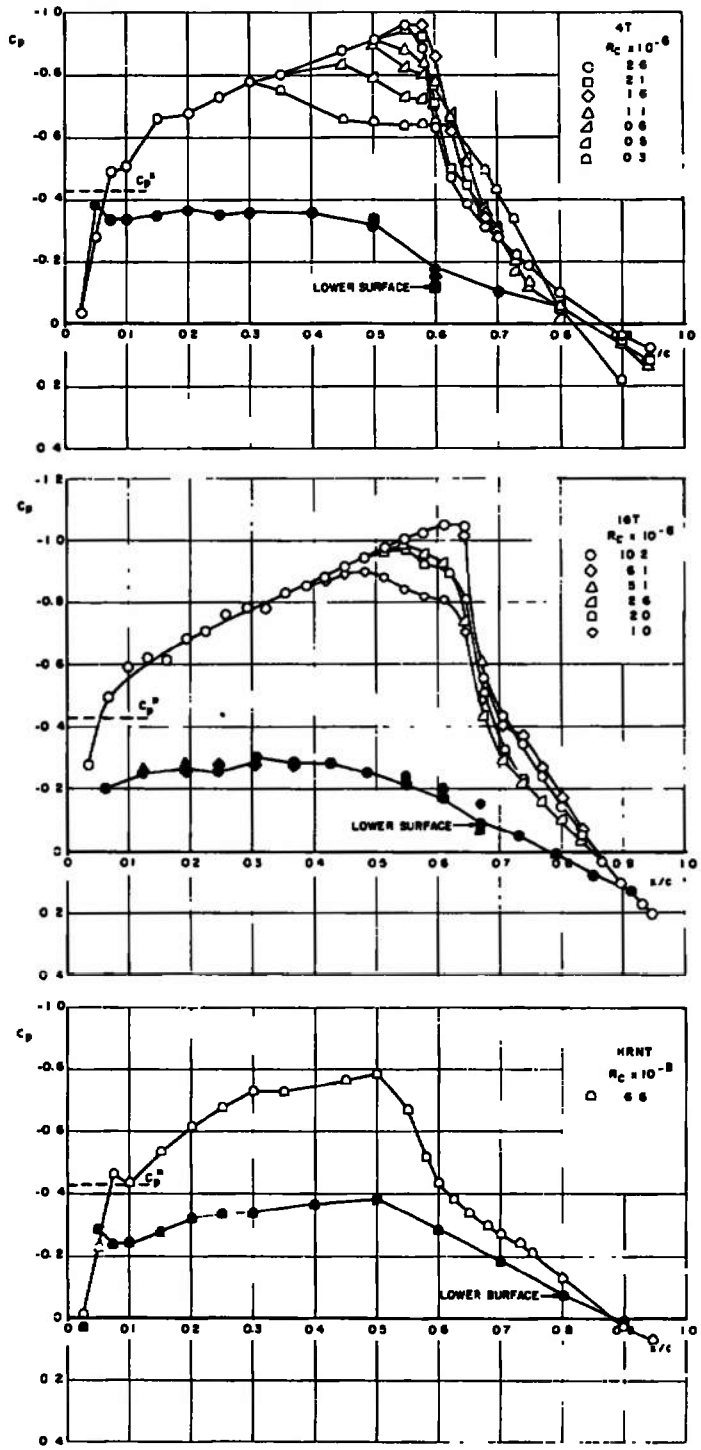

c. α = 2 deg

Fig. 18 Continued

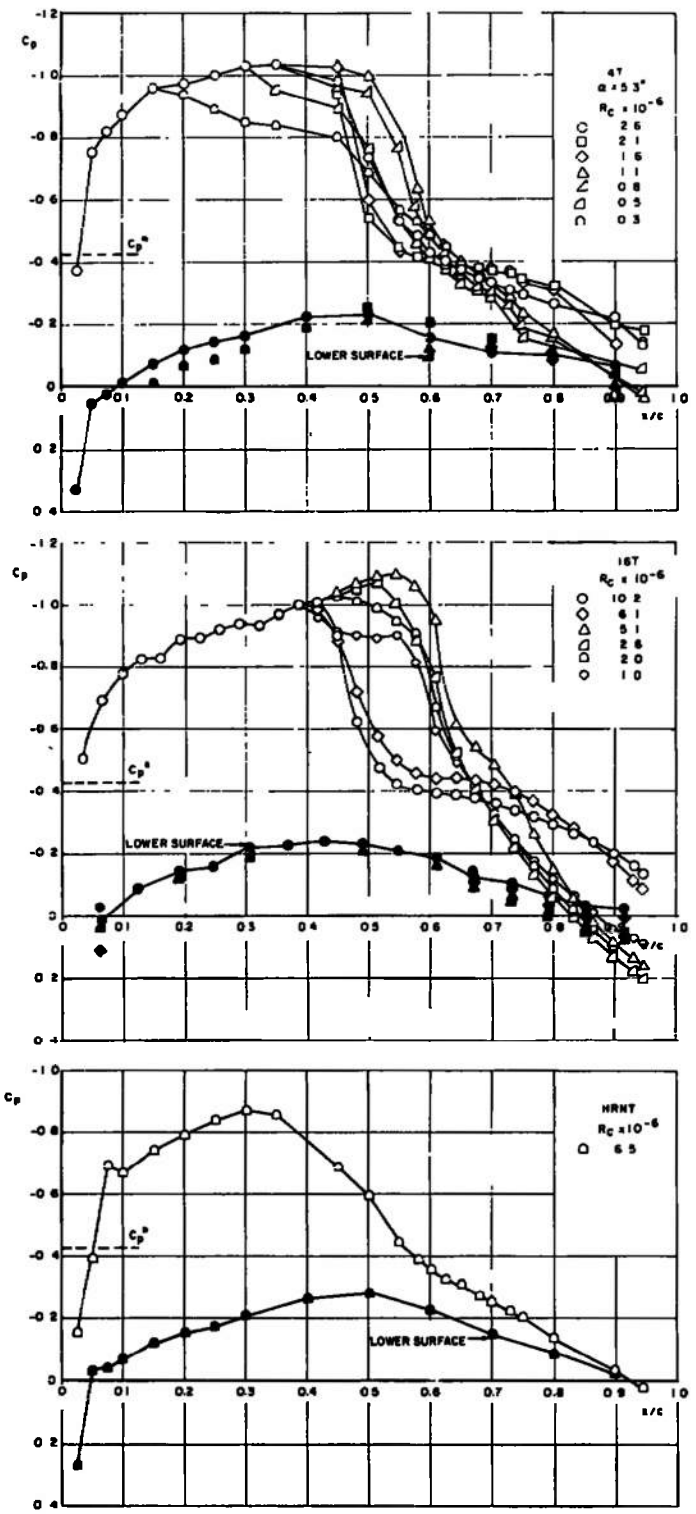

d. α = 4 deg

Fig. 18 Concluded

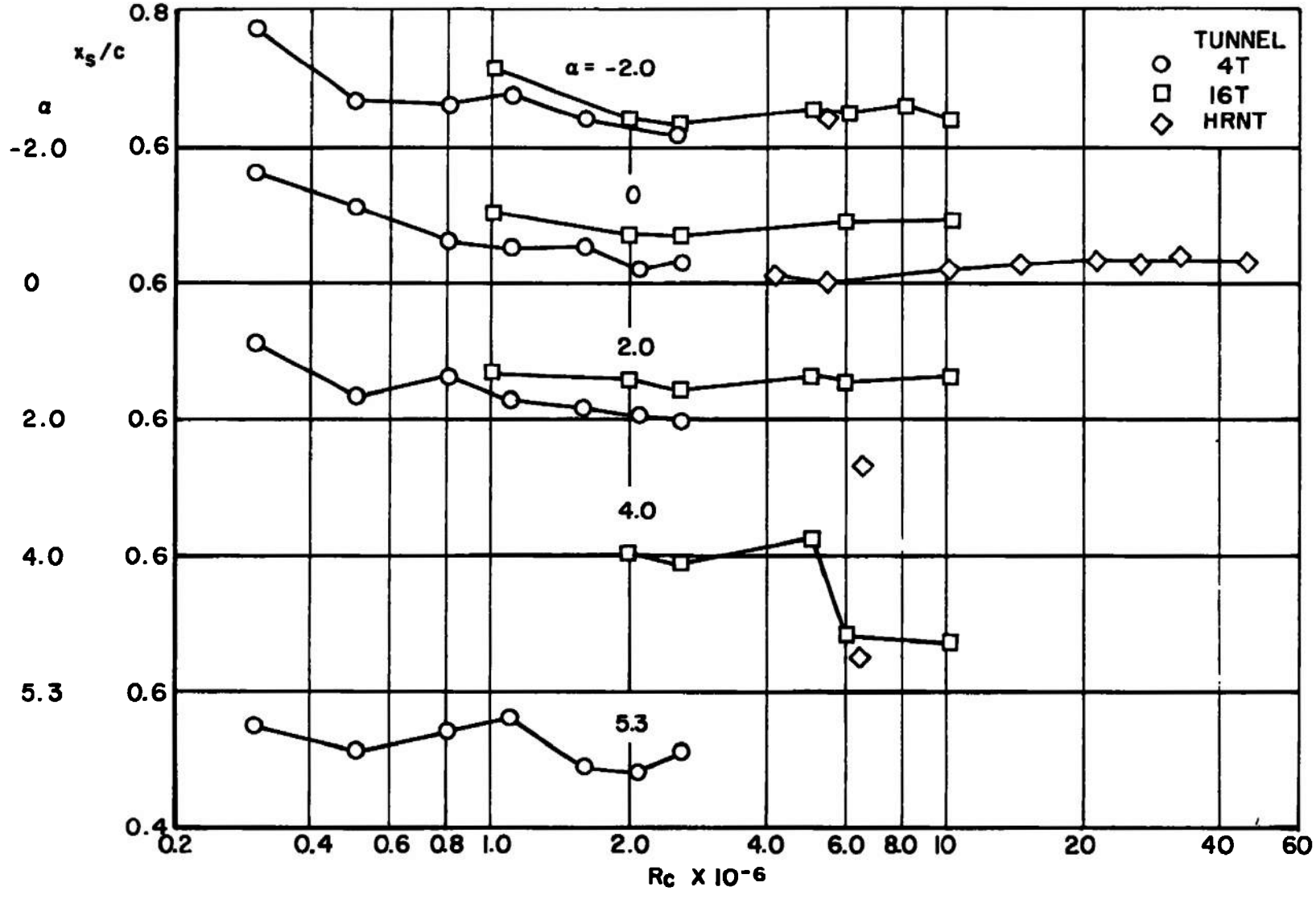

Fig. 19 Summary of Effect of Reynolds Number on the Shock Wave Location of the Upper Surface at M_∞ = 0.8 and α = -2 to 5.3 deg

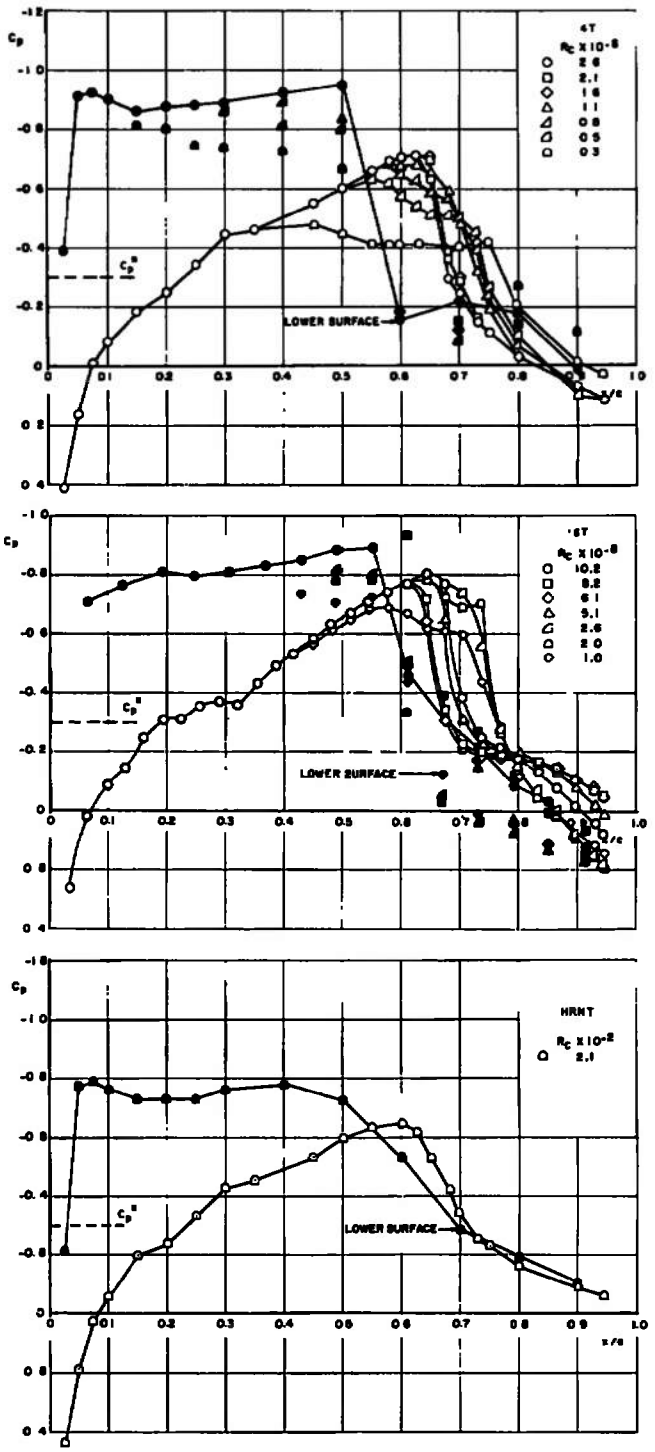

a. α = -2 deg

Fig. 20 Effect of Reynolds Number on the Pressure Distributions of the Airfoil Models in Various Tunnels at M_∞ = 0.85

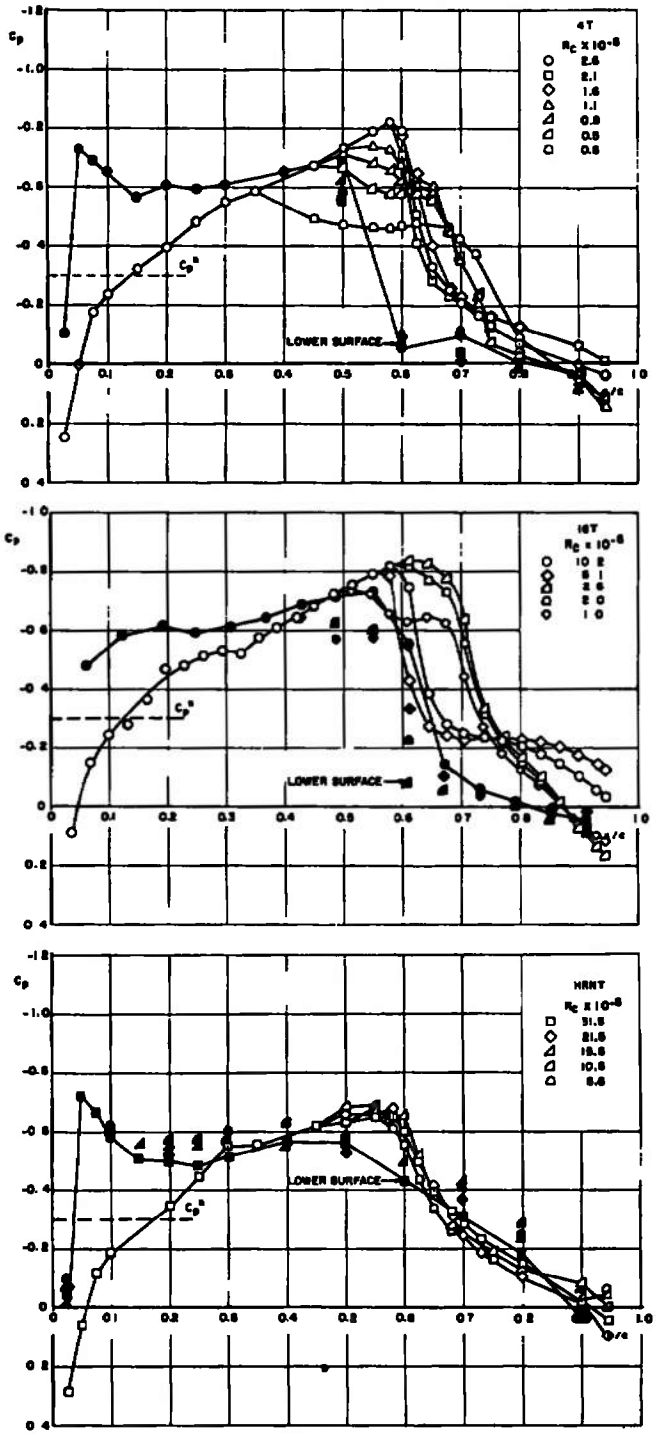

b. α = 0 deg

Fig. 20 Continued

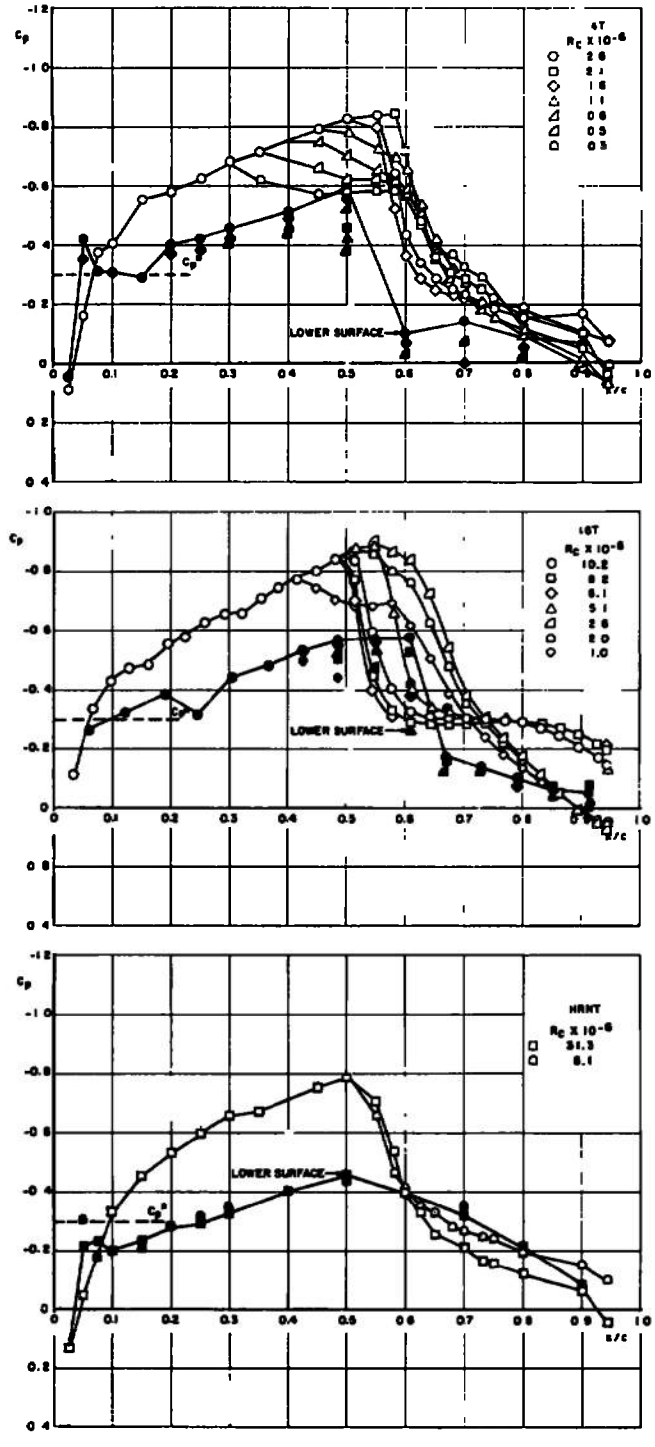

c. α = 2 deg

Fig. 20 Continued

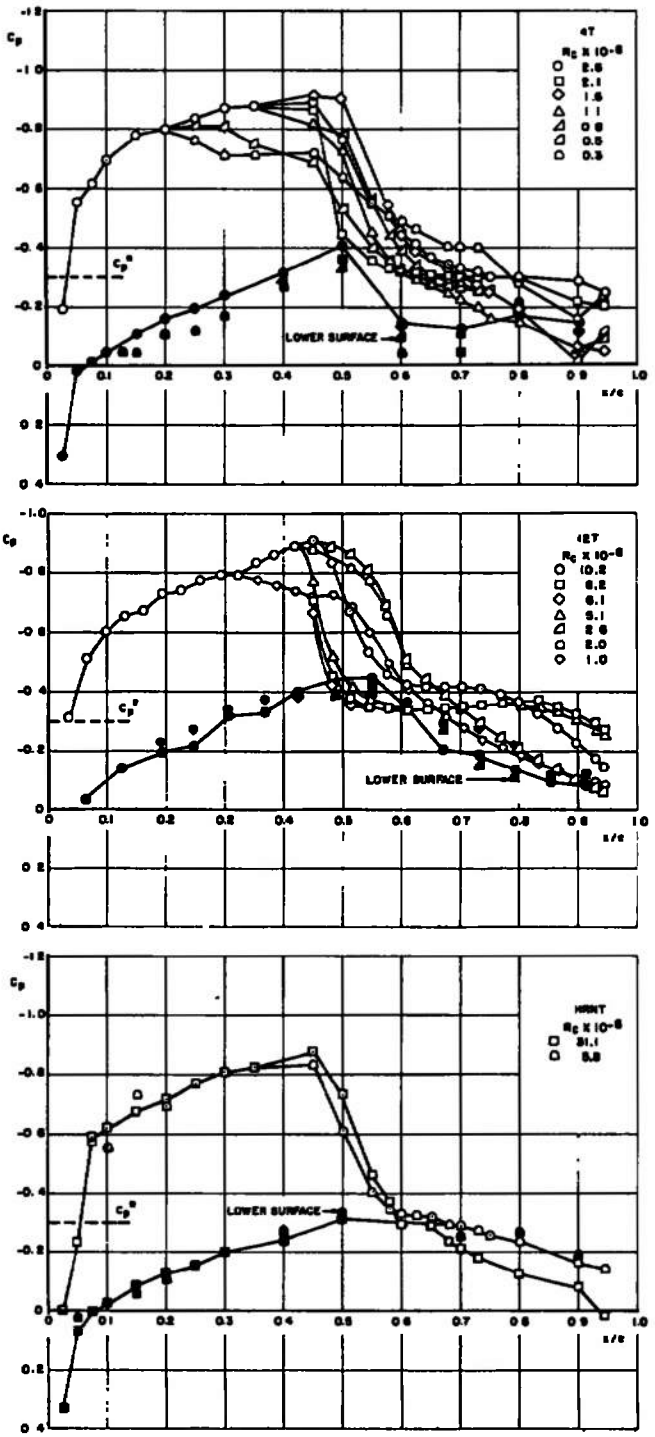

d. α = 4 deg
Fig. 20 Concluded

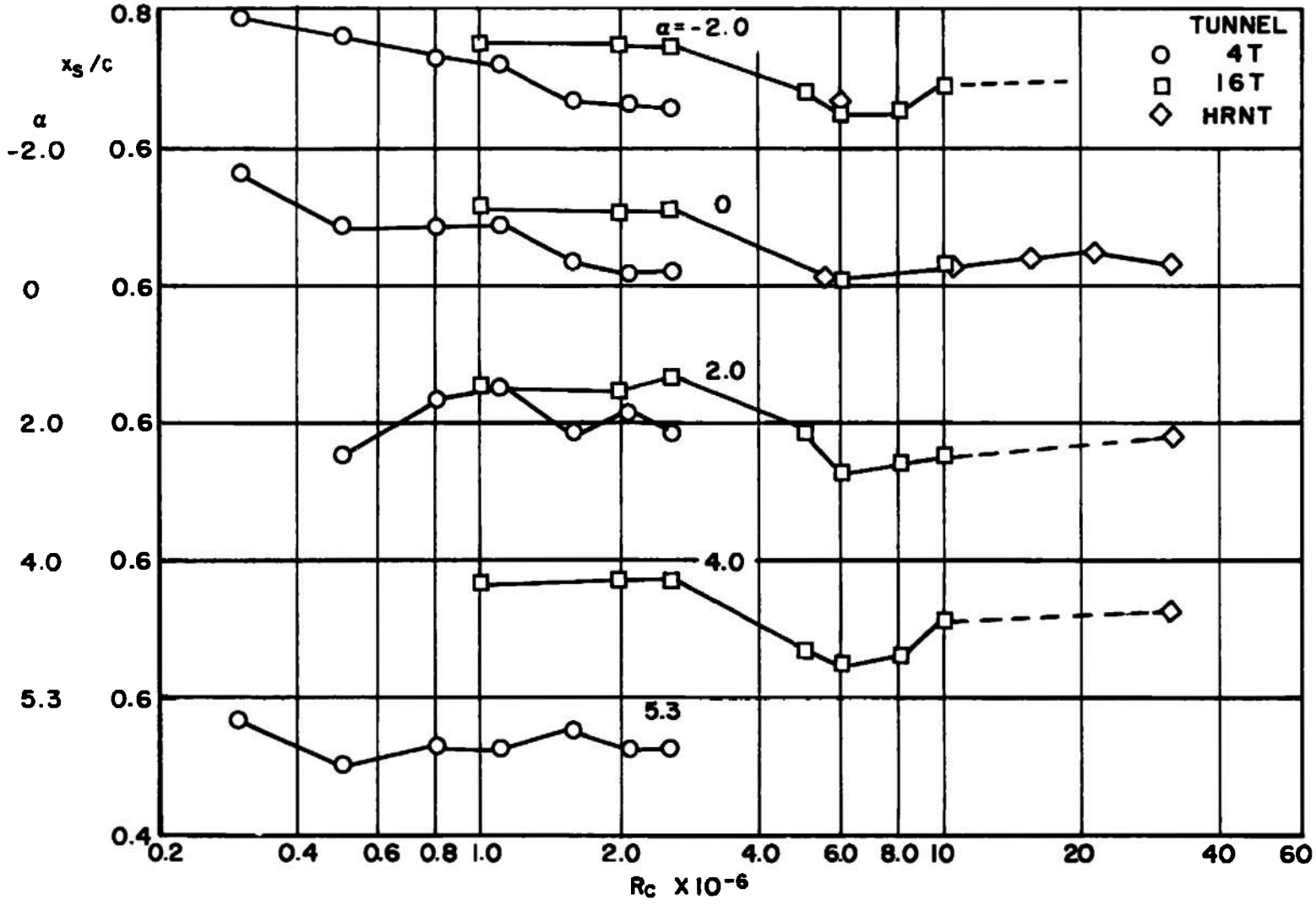

Fig. 21 Summary of Effect of Reynolds Number on the Shock Wave Location of the Upper Surface at M_∞ = 0.85 and α = -2 to 5.3 deg

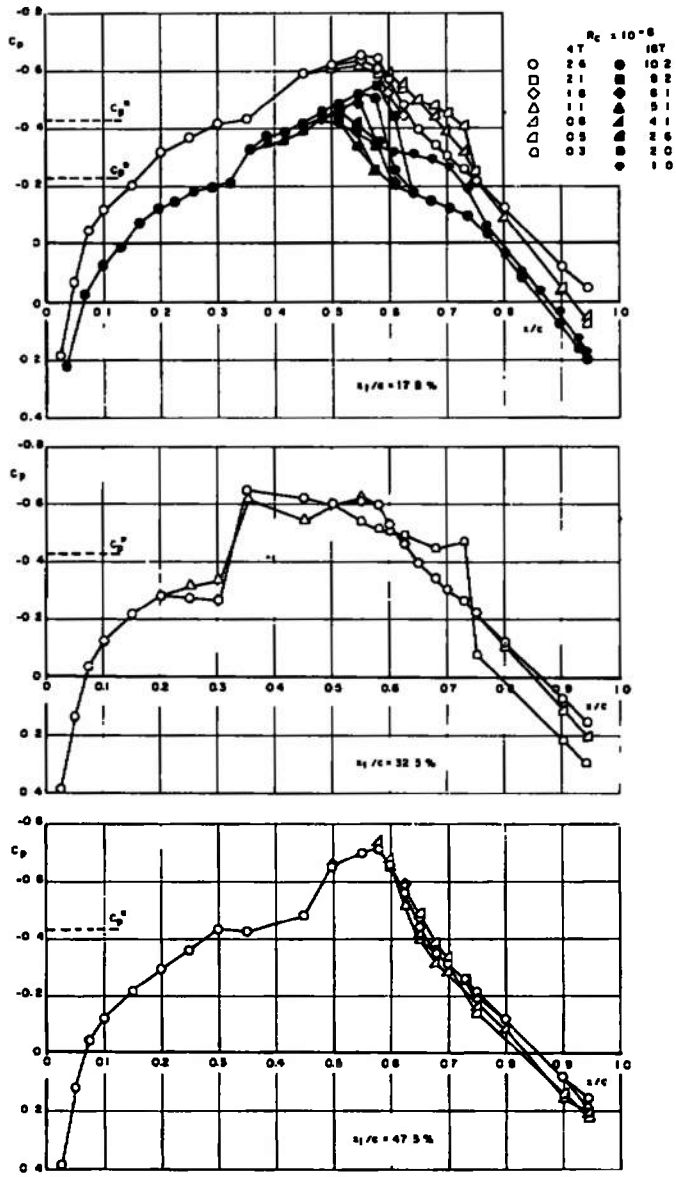

a. α = -2 deg

Fig. 22 Effect of Fixed-Transition Location on the Upper-Surface Pressure Distribution at M_∞ = 0.8 and R_c = 0.3 to 10.2 x 10^6

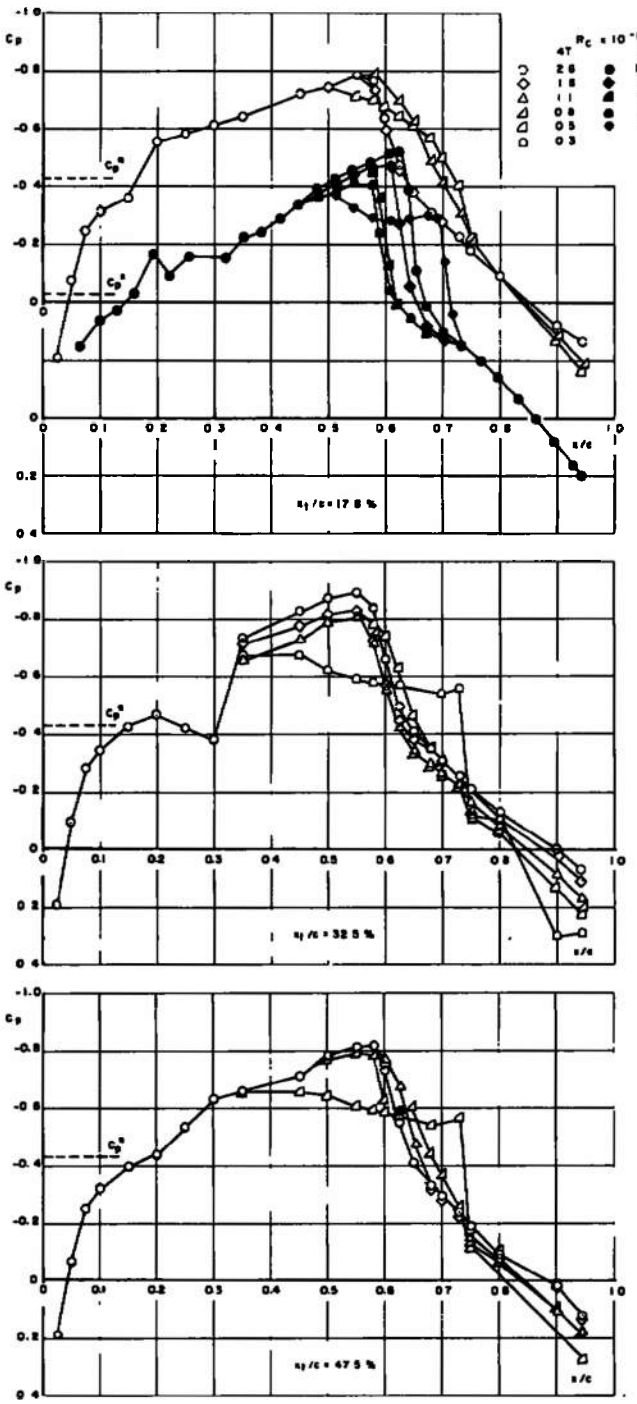

b. α = 0 deg
Fig. 22 Continued

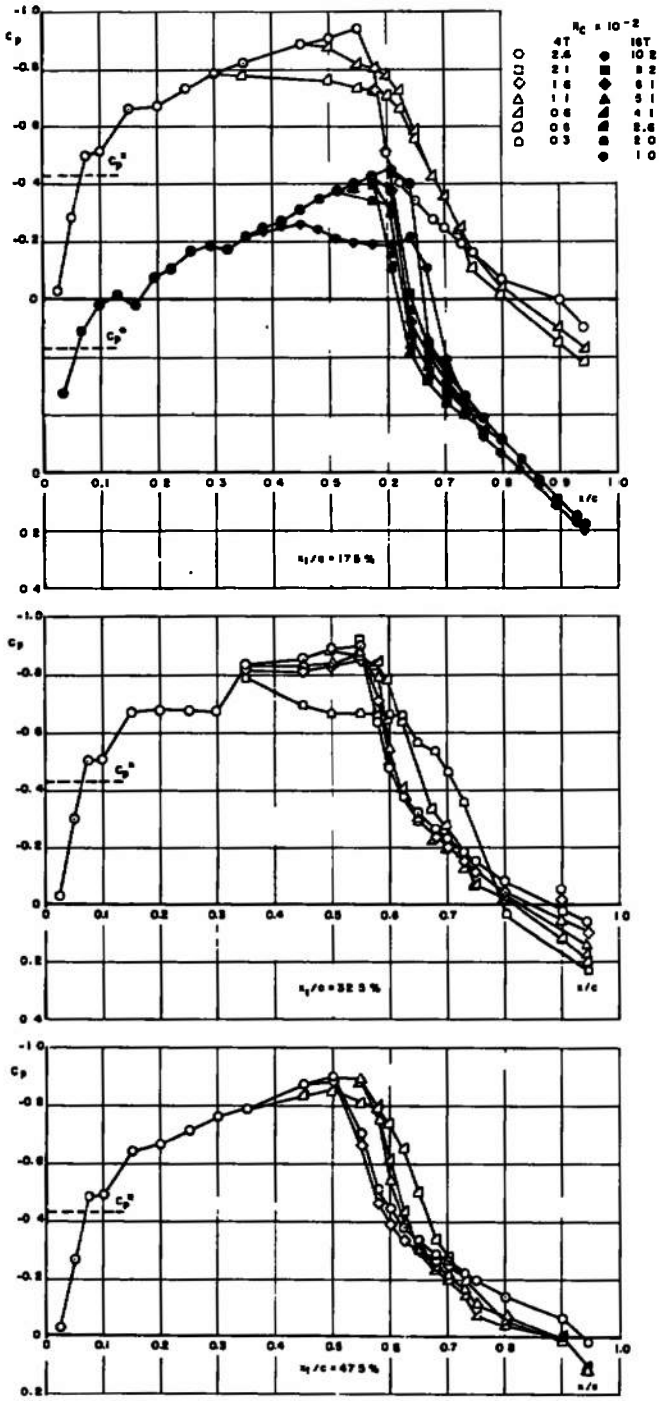

c. α = 2 deg
Fig. 22 Continued

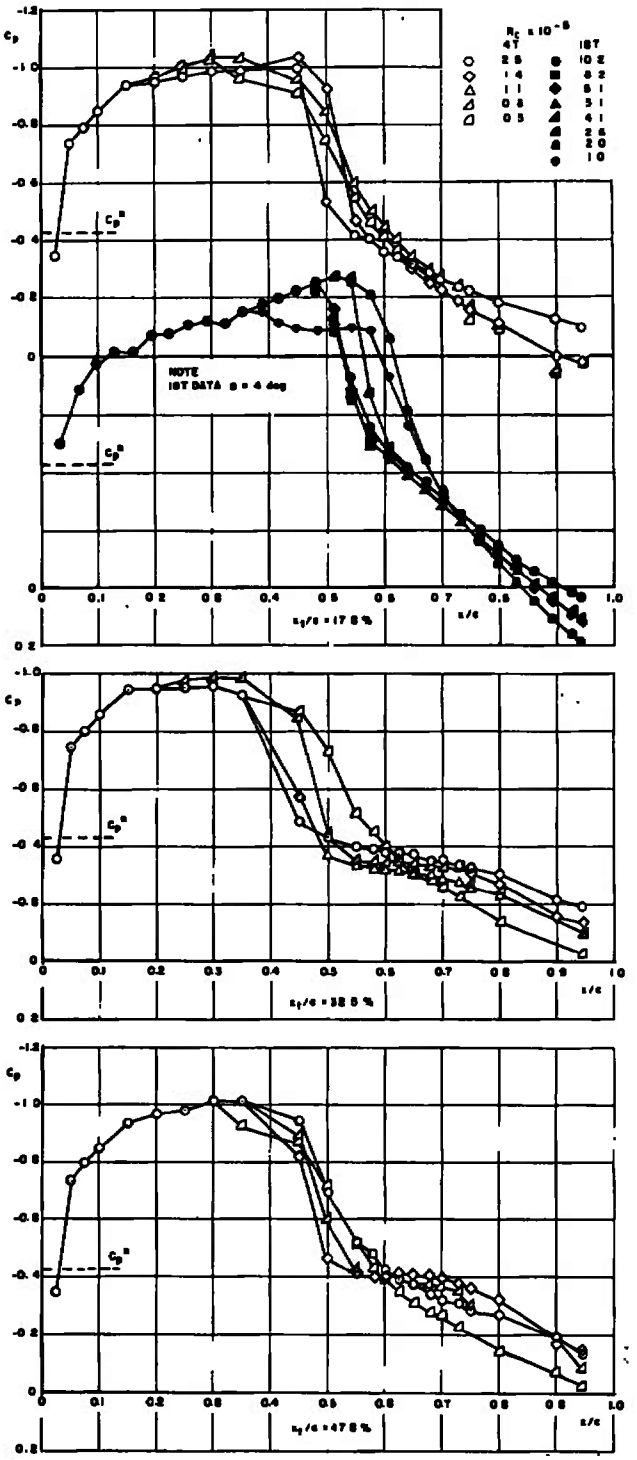

d. α = 5.3 deg

Fig. 22 Concluded

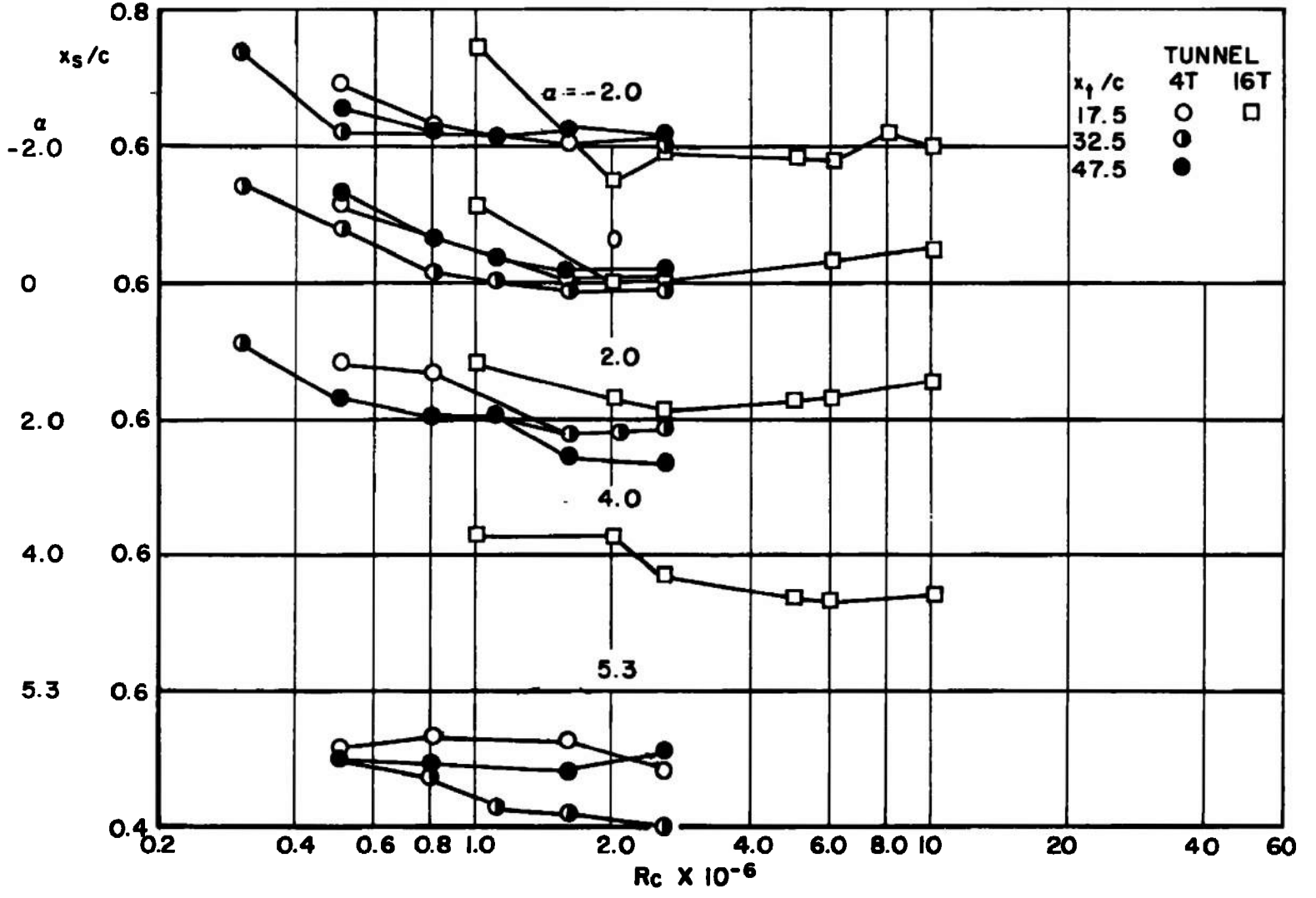

Fig. 23 Summary of Effect of Fixed-Transition Location on the Shock Wave Position of the Upper Surface at M_∞ = 0.8 and α = -2 to 5.3 deg

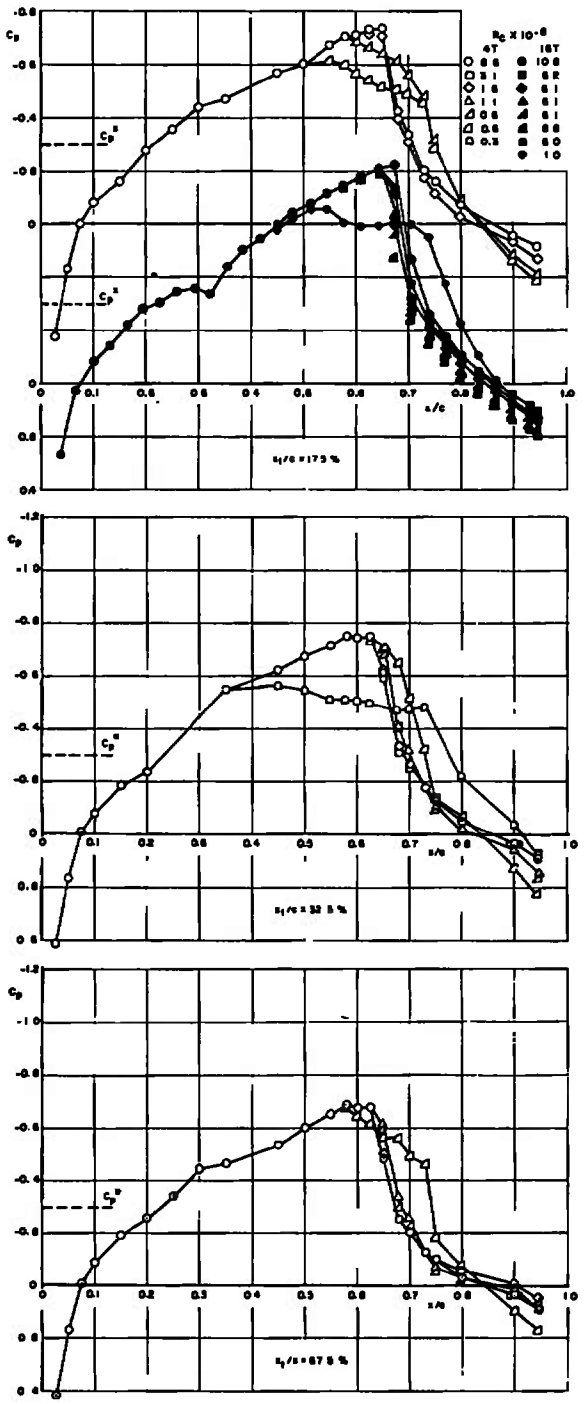

a. α = -2 deg

Fig. 24 Effect of Fixed-Transition Location on the Upper-Surface Pressure Distribution at M_∞ = 0.85 and R_c = 0.3 to 10.2 x 10^6

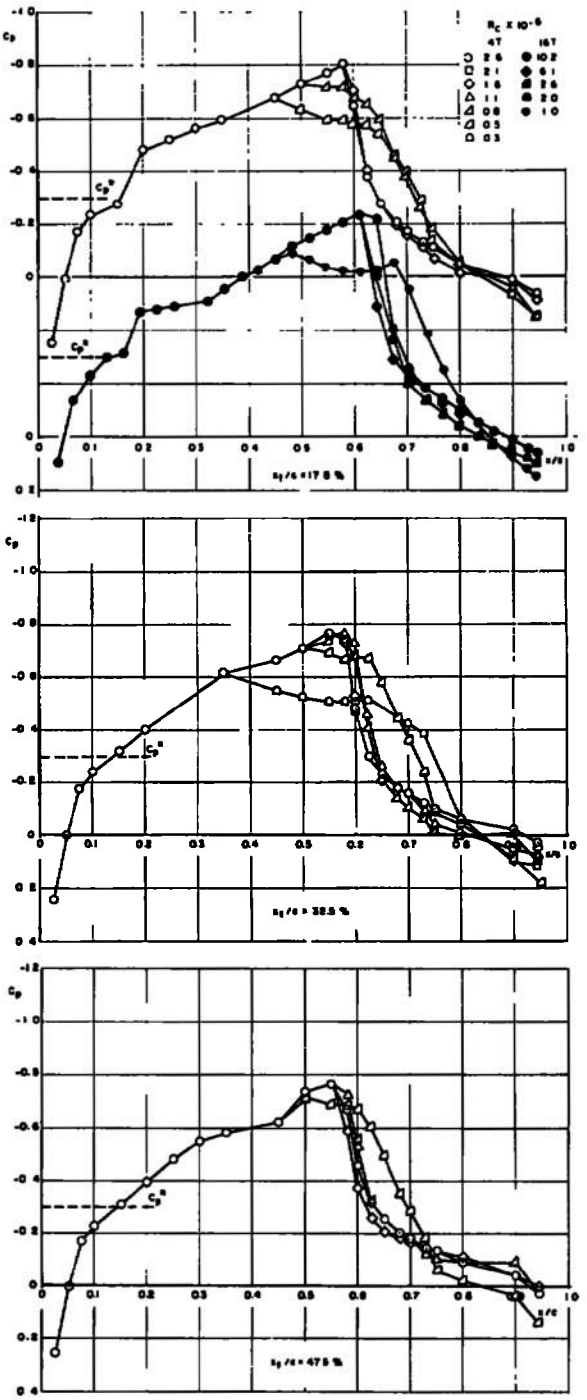

b. α = 0 deg
Fig. 24 Continued

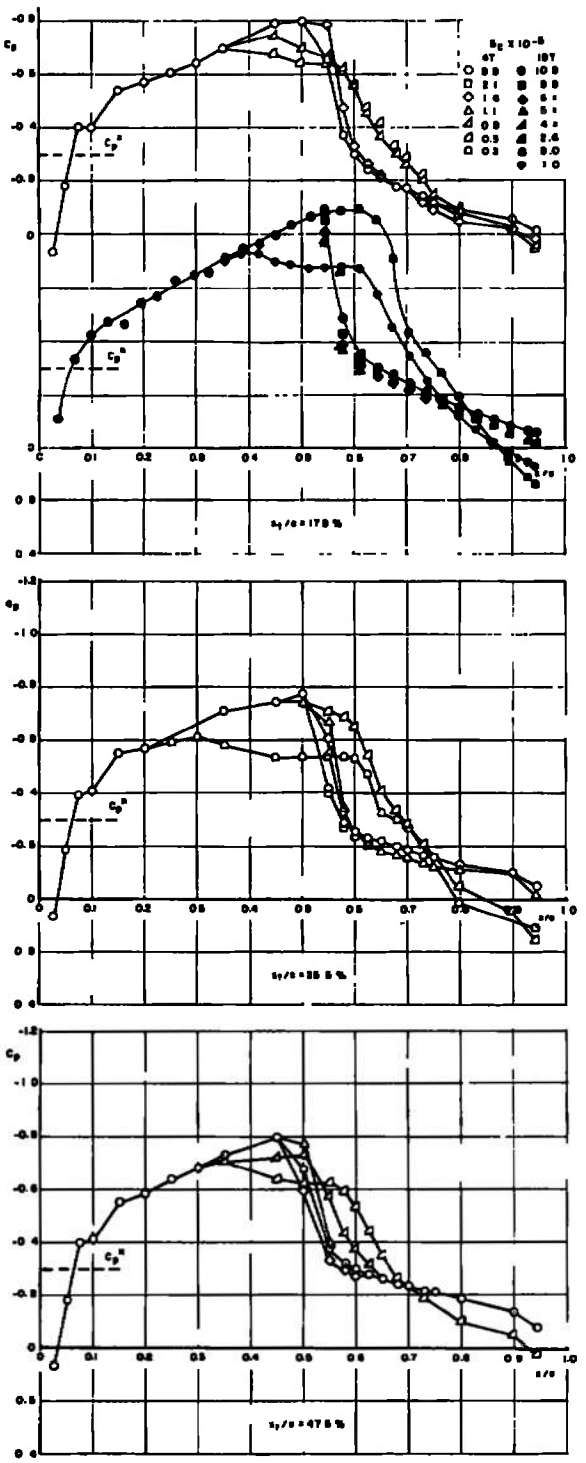

c. α = 2 deg

Fig. 24 Continued

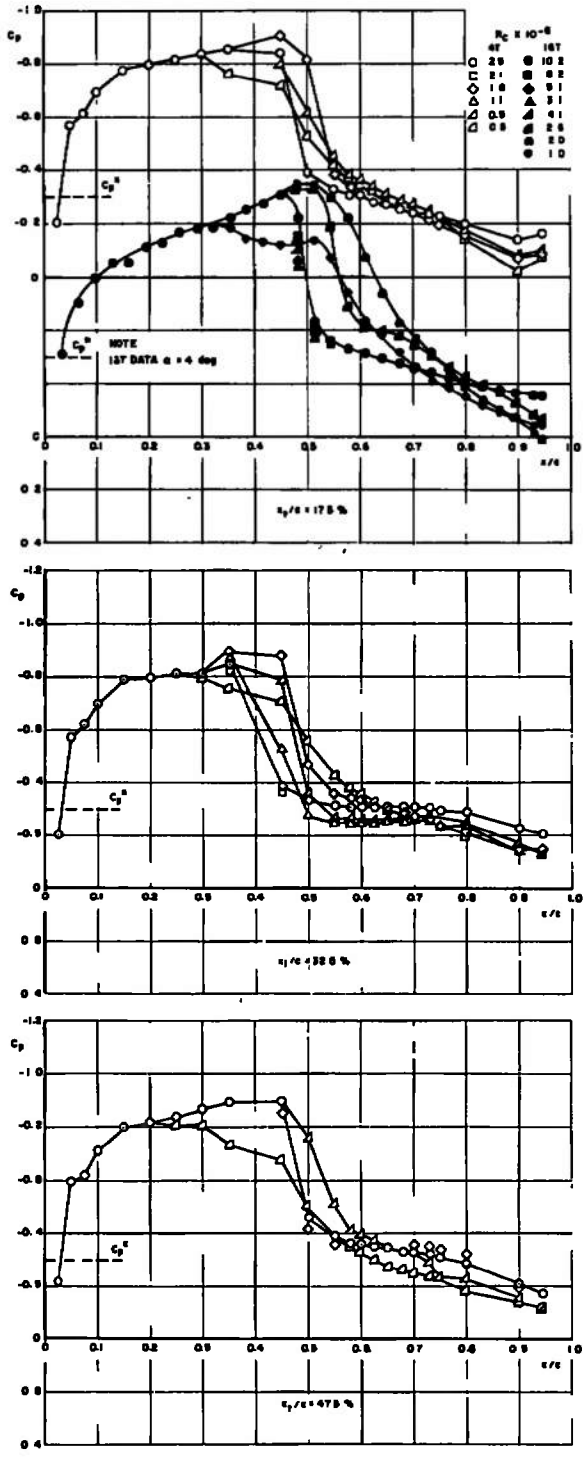

d. α = 5.3 deg
Fig. 24 Concluded

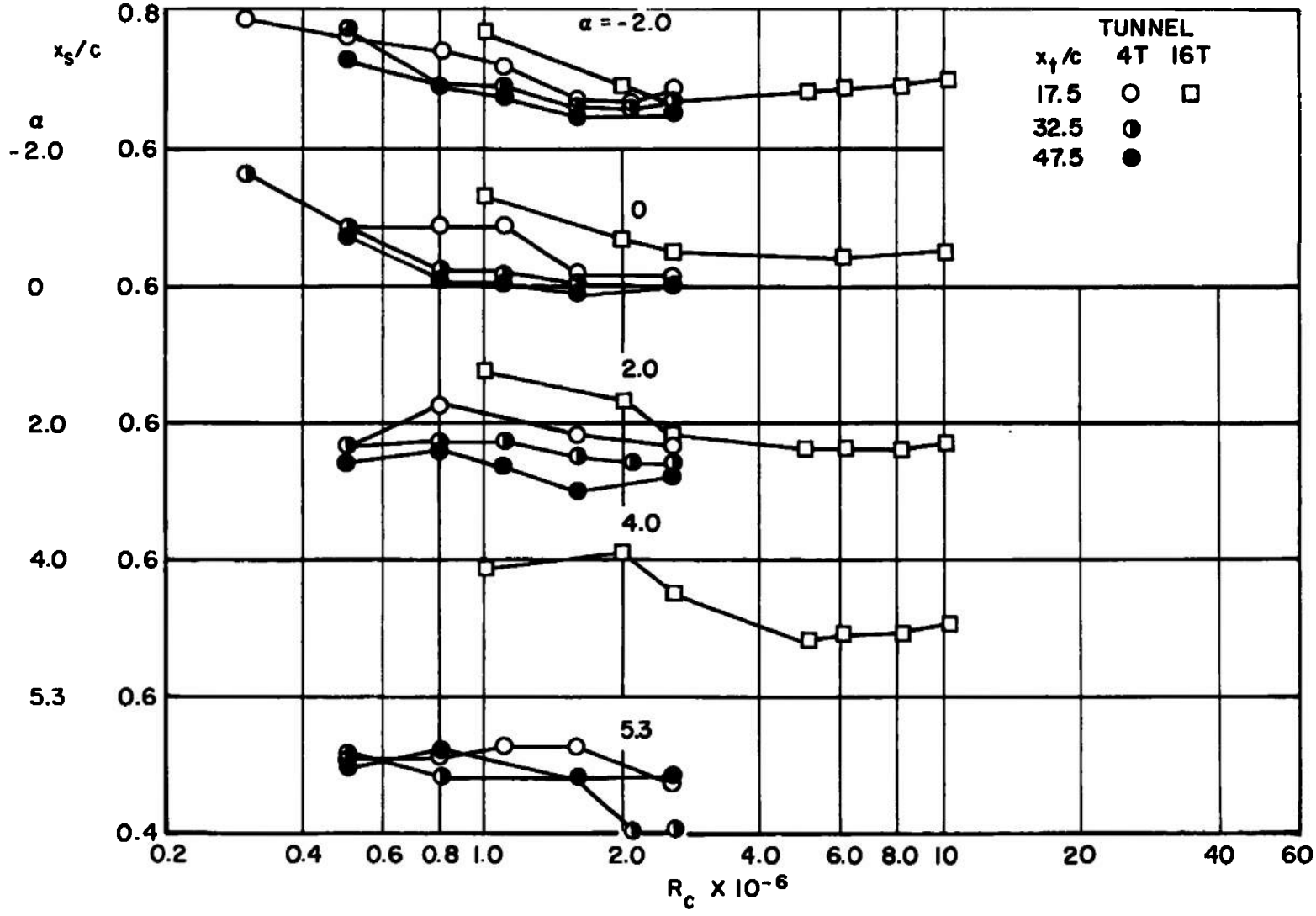

Fig. 25 Summary of Effect of Fixed-Transition Location on the Shock Wave Position of the Upper Surface at M_∞ = 0.85 and α = -2 to 5.3 deg

TABLE I
AIRFOIL SECTION CORRDINATES

UPPER SURFACE		LOWER SURFACE	
X/c	Z/c	X/c	Z/c
0.0003	0.0046	0.0005	-0.0032
0.0008	0.0064	0.0009	-0.0045
0.0013	0.0080	0.0017	-0.0063
0.0018	0.0092	0.0031	-0.0087
0.0053	0.0143	0.0059	-0 0119
0.0076	0.0168	0.0099	-0.0154
0.0112	0.0199	0.0165	-0.0194
0.0160	0.0233	0.0217	-0.0220
0.0233	0.0275	0.0373	-0.0273
0.0480	0 0375	0.0681	-0.0340
0.0728	0.0446	0.0936	-0.0377
0.0978	0.0500	0.1038	-0.0389
0.1178	0.0538	0.1242	-0.0410
0.1478	0.0583	0.1547	-0.0435
0.1979	0.0644	0.1750	-0.0448
0.2480	0.0688	0.2053	-0.0463
0.2980	0.0720	0.2557	-0.0482
0.3480	0.0741	0.3059	-0.0493
0.3979	0.0752	0.3560	-0.0495
0.4477	0.0752	0.4058	-0.0490
0.4974	0.0741	0.4554	-0.0478
0.5470	0.0720	0.5048	-0.0460
0.5965	0.0688	0.5541	-0 0436
0.6461	0.0646	0.6025	-0.0403
0.6962	0.0593	0.6521	-0.0365
0.7465	0.0530	0.6845	-0.0335
0.7967	0.0452	0.7247	-0.0304
0.8472	0.0360	0.7846	-0.0246
0.8976	0.0257	0.8341	-0.0197
0.9986	0.0018	0.8670	-0.0162
		0.8999	-0.0124
		0.9164	-0.0105
		0.9651	-0.0043
		0.9822	-0.0021

UNCLASSIFIED

Security Classification

DOCUMENT CONTROL DATA - R & D

(Security classification of title, body of abstract and indexing annotation must be entered when the overall report is classified)

1 ORIGINATING ACTIVITY (Corporate author)	2a. REPORT SECURITY CLASSIFICATION
Arnold Engineering Development Center Arnold Air Force Station, Tennessee 37389	UNCLASSIFIED
	2b. GROUP N/A

3 REPORT TITLE

TRANSONIC SCALING EFFECT ON A QUASI, TWO-DIMENSIONAL C-141 AIRFOIL MODEL

4 DESCRIPTIVE NOTES (Type of report and inclusive dates)

Final Report - February 1970 to June 1972

5 AUTHOR(S) (First name, middle initial, last name)

C. F. Lo and W. E. Carleton, ARO, Inc.

6 REPORT DATE	7a. TOTAL NO OF PAGES	7b. NO OF REFS
June 1973	69	11

8a. CONTRACT OR GRANT NO	9a. ORIGINATOR'S REPORT NUMBER(S)
b. PROJECT NO	AEDC-TR-73-61
c. Program Elements 64719F and 61102F	9b. OTHER REPORT NO(S) (Any other numbers that may be assigned this report)
d.	ARO-PWT-TR-73-13

10 DISTRIBUTION STATEMENT

Approved for public release; distribution unlimited.

11 SUPPLEMENTARY NOTES	12. SPONSORING MILITARY ACTIVITY
Available in DDC.	Arnold Engineering Development Center, Air Force Systems Command, Arnold AF Station, Tenn. 37389

13 ABSTRACT The transonic scaling effect of shock wave/boundary-layer interaction on a quasi, two-dimensional C-141 airfoil was investigated. Data were obtained from the AEDC Propulsion Wind Tunnel Facility Aerodynamic Wind Tunnel (4T) and Propulsion Wind Tunnel (16T) and from the NASA Marshall Space Flight Center High Reynolds Number Tunnel with 6-in.- and 24-in.-chord airfoils for a range of chord Reynolds numbers from 0.3 to 42 million and Mach numbers from 0.70 to 0.85. In addition to the investigation of the effect of Reynolds number on the airfoil pressure distribution, the effect of fixed boundary-layer transition was evaluated using grit-type transition strips on the airfoil surface. The significant parameters affecting the shock wave/boundary-layer interaction are identified. The data indicate that simulation of higher Reynolds number data on the C-141 airfoil model is feasible by use of a fixed-boundary-layer-transition strip.

DD FORM 1 NOV 65 1473

UNCLASSIFIED

Security Classification

14. KEY WORDS	LINK A		LINK B		LINK C	
	ROLE	WT	ROLE	WT	ROLE	WT
Reynolds number scaling						
boundary layer interaction						
shock waves						
transonic flow						
two-dimensional flow						
high Reynolds number simulation						

AFSC
Arnold AFS Tenn